

# 1 Minimizing the effects of Pb-loss in detrital and igneous U-Pb zircon 2 geochronology by CA-LA-ICP-MS

3  
4 Erin E. Donaghy<sup>1</sup>, Michael P. Eddy<sup>1</sup>, Federico Moreno<sup>2</sup>, Mauricio Ibañez-Mejía<sup>2</sup>

5 <sup>1</sup>Department of Earth, Atmospheric, and Planetary Sciences, Purdue University, West Lafayette, 47907, United  
6 States of America

7 <sup>2</sup>Department of Geosciences, University of Arizona, Tucson, 85721, United States of America  
8

9 *Correspondence to:* Erin E. Donaghy (edonaghy@purdue.edu)

10  
11 **Abstract.** Detrital zircon geochronology by laser ablation-inductively coupled plasma-mass spectrometry (LA-ICP-  
12 MS) is a widely-used tool for determining maximum depositional ages, sediment provenance, and reconstructing  
13 sediment routing pathways. Although the accuracy and precision of U-Pb geochronology measurements has improved  
14 over the past two decades, Pb-loss continues to impact the ability to resolve zircon age populations by biasing affected  
15 zircon toward younger apparent ages. Chemical abrasion (CA) has been shown to reduce or eliminate the effects of  
16 Pb-loss in zircon U-Pb geochronology, but has yet to be widely applied to large-n detrital zircon analyses. Here, we  
17 assess the efficacy of the chemical abrasion treatment on zircon prior to analysis by LA-ICP-MS and discuss the  
18 advantages and limitations of this technique in relation to detrital zircon geochronology. We show that i) CA does not  
19 systematically bias LA-ICP-MS U-Pb dates for thirteen reference materials that span a wide variety of crystallization  
20 dates and U concentrations; ii) CA-LA-ICP-MS U-Pb zircon geochronology can reduce, or eliminate, Pb-loss in  
21 samples that have experienced significant radiation damage; and iii) bulk CA prior to detrital zircon U-Pb  
22 geochronology by LA-ICP-MS improves the resolution of age populations defined by <sup>206</sup>Pb/<sup>238</sup>U dates  
23 (Neoproterozoic and younger) and increases the percentage of concordant analyses in age populations defined by  
24 <sup>207</sup>Pb/<sup>206</sup>Pb dates (Mesoproterozoic and older). The selective dissolution of zircon that has experienced high degrees  
25 of radiation damage suggests that some detrital zircon age populations could be destroyed or have their abundance  
26 significantly modified during this process. However, we did not identify this effect in either of the detrital zircon  
27 samples that were analyzed as part of this study. We conclude that pre-treatment of detrital zircon by bulk CA may be  
28 useful for applications that require increased resolution of detrital zircon populations and increased confidence that  
29 <sup>206</sup>Pb/<sup>238</sup>U dates are unaffected by Pb-loss.

## 30 31 1. Introduction

32 Detrital zircon U-Pb geochronology is a widely-used tool with a broad range of applications across multiple  
33 subdisciplines of geology. As the efficiency, accuracy, and precision of U-Pb geochronology measurements continue  
34 to improve (e.g., Carrapa, 2010; Gehrels, 2012; Gehrels, 2014; Pullen et al., 2014; Sundell et al., 2021), the production  
35 of large detrital zircon datasets by laser ablation-inductively coupled plasma-mass spectrometry (LA-ICP-MS) has  
36 become more common. In basin analysis and tectonics, these datasets are often used to determine sediment  
37 provenance, characterize source terranes, estimate maximum depositional ages, and reconstruct ancient sediment  
38 routing pathways (Fedo et al., 2003; Anderson 2005; Smith et al., 2023). The resulting data is typically interpreted  
39 using kernel density estimates (KDEs) or probability density plots (PDPs) and assessed by comparing the means,

40 heights, widths, and modes of peaks in detrital zircon age spectra using similarity/dissimilarity metrics. One factor  
41 that may limit the resolution of these peaks is Pb-loss which can smear zircon age populations toward younger apparent  
42 U-Pb dates. This issue may not bias data in which Pb-loss is a recent phenomenon provided that the  $^{207}\text{Pb}/^{206}\text{Pb}$  date  
43 is used for zircon crystallization. However, protracted or complicated histories of Pb-loss can make it difficult to  
44 interpret  $^{207}\text{Pb}/^{206}\text{Pb}$  dates (Nemchin and Cawood, 2005) and many labs only use this system to constrain a zircon  
45 crystallization date if it is concordant. The precision of the  $^{207}\text{Pb}/^{206}\text{Pb}$  chronometer also typically limits its use to  
46 Mesoproterozoic and older zircon. The most precise date for Neoproterozoic or younger zircon is generally obtained  
47 with the  $^{206}\text{Pb}/^{238}\text{U}$  chronometer and these dates are more susceptible to open-system behavior. Zircon age populations  
48 that are affected by Pb-loss in this age range can be difficult to identify since Pb-loss trajectories closely follow  
49 Concordia and may result in analyses that are concordant within analytical uncertainty but have spuriously young  
50  $^{206}\text{Pb}/^{238}\text{U}$  dates. This is especially problematic for the estimation of maximum depositional ages (MDAs) in detrital  
51 zircon datasets where age estimations utilize low-n clusters of the youngest zircon ages (Dickinson and Gehrels, 2009;  
52 Herriott et al., 2019; Coutts et al., 2019; Sharman et al., 2020; Vermeesch, 2021). The effect of Pb-loss on detrital  
53 zircon analyses is consequently two-fold. It reduces the number of concordant Mesoproterozoic and older zircons,  
54 making populations in this age range more difficult to identify, and it will cryptically smear Neoproterozoic and  
55 Phanerozoic zircon age populations along concordia toward spuriously young dates, making it difficult to resolve  
56 differences between distinct but similarly aged populations.

57         While high temperature metamorphism may lead to zircon recrystallization and partial, or total, resetting of  
58 the U-Pb system, most Pb-loss in zircon that is hosted in sedimentary strata represents a low temperature process.  
59 Damage to the zircon crystal lattice occurs during each alpha emission along the  $^{238}\text{U}$ ,  $^{235}\text{U}$ , and  $^{232}\text{Th}$  decay chains as  
60 the heavy nucleus recoils (Bateman, 1910; Dickin, 2005; Nasdala et al., 2005; Reiners, 2005). At temperatures below  
61 200°C this damage cannot anneal and begins to accumulate (Marsellos and Garver, 2010; Ginster et al., 2019). Areas  
62 where high levels of damage have accumulated are then susceptible to Pb-loss (Chakoumakos et al., 1987; Mattinson  
63 et al., 1994; Garver and Kamp, 2002; Widmann et al., 2019; McKanna et al., 2023). The mechanisms through which  
64 Pb becomes mobile in metamict zircon grains remain understudied, but likely include mobility in low-temperature  
65 aqueous fluids (Goldich and Mudrey, 1972; Black, 1987; Kramers et al., 2009; Keller et al., 2019), which allows water  
66 to penetrate highly radiation damaged zircon and mobilize radiogenic Pb by changing its redox state (Kramers et al.,  
67 2009). Thus, the zircons that are most susceptible to Pb-loss at low temperatures are those that spend long durations  
68 at shallow crustal levels and encounter low-temperature aqueous fluids, both of which are conditions seen by detrital  
69 zircon hosted in sedimentary basins.

70         The chemical abrasion method, in which thermally annealed zircon is partially dissolved in hydrofluoric acid  
71 (HF) prior to analysis has been shown to successfully mitigate low-temperature Pb-loss (e.g., Mundil et al., 2004;  
72 Mattinson, 2005; Widmann et al., 2019; Sharman and Malkowski, 2023) and is widely used in isotope dilution-thermal  
73 ionization-mass spectrometry (ID-TIMS) U-Pb zircon geochronology (*see reviews in* Schoene, 2014; Schaltegger et  
74 al., 2015). The technique likely benefits analyses in two ways. First, it selectively dissolves zones of the zircon crystal  
75 that have experienced extensive radiation damage and possible Pb-loss (Widmann et al., 2019; McKanna et al., 2023).  
76 Second, the partial dissolution process dissolves inclusions that may harbor non-radiogenic Pb, leading to a higher

77 proportion of zircon-hosted radiogenic Pb (Pb\*) in the measured analysis. Over the last decade, several groups have  
78 analyzed chemically abraded zircon by LA-ICP-MS and shown that this approach can successfully mitigate Pb-loss,  
79 and results in increased concordance, precision, and, presumably, accuracy of U-Pb dates (Crowley et al., 2014; Von  
80 Quadt et al., 2014). These results suggest that chemical abrasion prior to large-n detrital zircon analyses may also be  
81 useful when the resolution of closely spaced Neoproterozoic and Phanerozoic peak age populations is desired or when  
82 high degrees of discordance obscure the interpretation of Mesoproterozoic and older age populations. Here, we assess  
83 the benefits and drawbacks of this pre-treatment with a particular focus on whether the resolution of younger zircon  
84 age populations is increased, whether it improves concordance for Precambrian detrital zircon populations, and/or  
85 whether the selective removal of metamict zircon will bias age populations.

86

## 87 **2. U-Pb Zircon Geochronology Approach and Methods**

88 We have divided our study into three distinct parts. First, we compare chemically abraded and untreated  
89 zircon from 13 zircon reference materials (Table 1) to test whether chemical abrasion systematically biases U-Pb dates  
90 analyzed by LA-ICP-MS. Crowley et al. (2014) demonstrated that chemically abraded zircon ablate more slowly and  
91 experience greater down-hole fractionation than untreated zircon. These differences are likely related to changes in  
92 the ability of the laser to couple with zircon that has been etched by the chemical abrasion process. While no negative  
93 effects of chemical abrasion were seen in Crowley et al. (2014) or von Quadt et al. (2014), provided that chemically  
94 abraded reference materials were used for instrument calibration, we have expanded the age range of reference zircon  
95 analyzed to encompass 28.5 – 3467 Ma. This increased age range of the tested reference materials provides a more  
96 complete understanding of LA-ICP-MS U-Pb systematics on chemically abraded zircon and whether a single primary  
97 reference material can be used to calibrate the instrument for a wide range of zircon dates. Second, we assess the  
98 ability of chemical abrasion to mitigate Pb-loss in an igneous sample that has experienced substantial radiation damage  
99 by comparing chemically abraded and non-chemically abraded  $^{206}\text{Pb}/^{238}\text{U}$  LA-ICP-MS zircon analyses to a newly  
100 produced CA-ID-TIMS reference date for a Mesoproterozoic granite. Finally, we assess how CA affects detrital zircon  
101 (DZ) age spectra by comparing chemically abraded and untreated aliquots of two detrital samples. One sample is  
102 Cenozoic in age and contains both Phanerozoic (100-300 Ma) and Precambrian (1000-1200 Ma) zircon age  
103 populations, whereas the second sample is Proterozoic and contains zircon age populations between 2000-3500 Ma.

104

### 105 **2.1 Methods for Thermal Annealing and Chemical Abrasion**

106 All chemically abraded zircon aliquots were treated at Purdue University following methods modified from  
107 Mattinson (2005) and similar to those described in Eddy et al. (2019). Zircon separates were first thermally annealed  
108 in quartz crucibles for 60 hours at 900°C in a muffle furnace and then loaded in 3 mL saviillex hex beakers with ~1  
109 mL of 28M HF and 0.1 mL of 8M HNO<sub>3</sub> for bulk chemical abrasion. Four hex beakers were then stacked in the PTFE  
110 liner for a 125 mL Parr acid dissolution vessel. To ensure vapor exchange during partial dissolution a small hole was  
111 drilled through each beaker cap. The fully assembled Parr acid dissolution vessel was then held at 210°C for 12 hours.  
112 Once the chemical abrasion process was completed, the leachate was removed from each beaker using a pipette and  
113 the zircons were rinsed three times with H<sub>2</sub>O. Chemically abraded aliquots were then sent to the University of Arizona  
114 LaserChron Center (ALC) for mounting and LA-ICP-MS analyses. Methods for chemical abrasion of zircon prior to

115 the ID-TIMS analyses reported in this paper are similar to those described above, except individual zircon were  
 116 chemically abraded in 200  $\mu$ L Ludwig style microcapsules and repeatedly rinsed in distilled 7M HCl and ultrapure  
 117 H<sub>2</sub>O prior to spiking and complete dissolution.  
 118

**Table 1.** Zircon reference materials for U-Pb isotopic analyses

Name	ID-TIMS age (Ma)	2 $\sigma$	References	Host lithology	Quantity
Fish Canyon Tuff	28.476	0.029	Schmitz and Bowring (2001) <sup>b, c</sup>	Dacite	Unlimited
GHR1	48.106	0.023	Eddy et al. (2019) <sup>b</sup>	Rapakivi Granite	Unlimited
49127	136.6		Gehrels et al. (2008) <sup>b</sup>		Uncertain
Plesovice	337.13	0.37	Slama et al. (2008) <sup>a</sup>	Potassic Granulite	Unlimited
Temora 2	418.37	0.14	Mattinson (2010) <sup>a</sup>	Gabbro	Unlimited
R33	420.53	0.16	Mattinson (2010) <sup>a</sup>	Monzodiorite	Unlimited
SLM	563.5	3.2	Gehrels et al. (2008) <sup>b</sup>	Single Crystal	Limited
SLF	555.86	0.68	Wang et al. (2022) <sup>b</sup>	Single Crystal	Limited
91500	1065.4	0.3	Wiedenbeck et al. (1995) <sup>b</sup>	Single Crystal	Limited
FC1	1098.47	0.16	Mattinson (2010) <sup>a</sup>	Gabbro	Unlimited
Oracle	1434	8	Gehrels et al. (2008) <sup>b</sup>	Granite	Unlimited
QGNG	1851.6	0.6	Black et al. (2004) <sup>b</sup>	Quartz gabbro gneiss	Uncertain
OG1	3467.05	0.63	Stern et al. (2009) <sup>a</sup>	Diorite	Unlimited

<sup>a</sup> Chemical abrasion CA-ID-TIMS

<sup>b</sup> Traditional ID-TIMS

<sup>c</sup>CA-ID-TIMS analyses by Wotzlaw et al. (2013) show significant age dispersion in Fish Canyon Tuff relative to original U-Pb ID-TIMS date of Schmitz and Bowring (2001).

119

120

## 121 2.2 LA-ICP-MS Zircon U-Pb Geochronology

122 Zircon aliquots were mounted in 2.5-cm-diameter epoxy plugs, polished, and imaged by

123 cathodoluminescence using a Hitachi 3400N SEM and a Gatan Chroma CL system prior to analysis by LA-ICP-MS.

124 Chemically abraded zircon were only mounted with chemically abraded zircon reference materials, while untreated

125 zircon aliquots were mounted with untreated reference materials. U-Pb isotopic analyses were obtained via LA-ICP-

126 MS using a Thermo Element2 single-collector ICP-MS coupled with a Teledyne Photon Machines Analyte G2

127 excimer laser at the ALC. The diameter of the laser spot was set to 30 microns. Elemental- and mass-dependent

128 instrumental fractionation were corrected by bracketing unknown analyses with analyses of primary reference material

129 FC1 following the methods described in Pullen et al. (2018). Please see supplementary Table S23 for tuning

130 parameters for the laser and mass spectrometer. Only chemically abraded primary reference materials were used for

131 calibration of chemically abraded samples and only untreated primary reference materials were used for untreated

132 samples following the recommendations of Crowley et al. (2014). Bracketing of secondary and tertiary reference

133 materials occurred every 10-11 analyses with primary reference materials (FC1, SLF/SLM, R33) for the round-robin

134 comparison of zircon reference materials, every 2-3 analyses for igneous zircon analyses, and every 5 analyses for

135 detrital zircon samples. Data reduction was completed using an in-house Matlab script, AgeCalcML v.1.42 (Sundell

136 et al., 2021). This program allows the user to filter data by maximum <sup>206</sup>Pb/<sup>238</sup>U and/or <sup>207</sup>Pb/<sup>206</sup>Pb uncertainty

137 (typically set to 10%), reverse discordance (typically 5%), and normal discordance (typically 20%). For the purposes  
138 of this study, we de-activated all uncertainty and discordance filters in AgeCalcML and all isotopic data measured via  
139 LA-ICP-MS that is clearly from ablated zircon are reported in Tables S1-S13. However, age interpretations of igneous  
140 and detrital zircon data use filtered data (Tables S16-S21).

141 Uranium concentrations (ppm) reported from routine U-Pb LA-ICP-MS zircon analyses at ALC are  
142 semiquantitative and calibrated by bracketing unknowns with analyses of reference materials with a known average  
143 U concentration. However, since chemical abrasion selectively dissolves high-uranium zones, and thus modifies the  
144 average U concentration of reference materials by an unquantified amount, the reported U concentration values for  
145 reference materials analyzed by traditional (non-CA) ID-TIMS may no longer be valid. We found that the primary  
146 reference material SLF had homogenous  $^{238}\text{U}$  cps (counts per second) within individual sessions (Figs. S15-S17) for  
147 both the CA and non-CA runs. We interpret this to mean that SLF has a homogenous U concentration (and radiation  
148 damage) and that any differences in  $^{238}\text{U}$  cps for SLF between different analytical sessions are related to changes in  
149 the instrument's sensitivity. As such, we normalize the  $^{238}\text{U}$  cps for all other grains analyzed in each session to the  
150 average  $^{238}\text{U}$  cps of SLF across all sessions. Given the potential difference between chemically abraded and untreated  
151 SLF U concentrations, we did this correction independently for treated and untreated grains. Since we do not have U  
152 concentration values for treated and untreated SLF, we center our discussions on relative differences in U  
153 concentration as estimated using the intensity (in cps) of the  $^{238}\text{U}$  beam, rather than quantifying U concentrations.

154 We used Saylor and Sundell (2016) DZstats program to complete a quantitative assessment of the similarity  
155 between treated and untreated aliquots. This program implements five tests to compare large-n geochronologic or  
156 thermochronologic datasets. The tests used in this study are similarity, likeness, and cross-correlation. Results from  
157 all five tests are shown in Supplemental Table S22 for both detrital zircon samples. The similarity coefficient measures  
158 if two samples have similar modal sub-intervals as well as similar proportions of components in each one of those  
159 modes. A value for similarity equal to 1 indicates the samples are identical in both peak modes and proportions,  
160 whereas 0 indicates there is no match between modes and proportions (Saylor and Sundell, 2016). This test is useful  
161 in assessing the number of peak age populations (similar mode intervals) and how peak heights (proportion of  
162 components in each mode) change between two samples. The cross-correlation coefficient is also sensitive to the  
163 presence or absence of peak ages, but also changes due to the relative magnitude and shape of peaks. If a sample  
164 shared the same peak ages, peak shapes, and magnitude of peaks, it would have a  $R^2$  value of 1. If no peak ages, peak  
165 shapes, and magnitude of peaks are shared, the  $R^2$  value would be 0 (Saylor and Sundell, 2016). Likeness is the  
166 complement of the area of mismatch between two detrital zircon spectra, or more simply put the degree of "sameness"  
167 between detrital zircon age populations (Satkoski et al., 2013). Thus, the likeness test compares the degree of overlap  
168 between pairs of PDPs and is a measure of resemblance between proportions of two populations with overlapping  
169 ages (Gehrels, 2009; Satkoski et al., 2013). Values of likeness that approach 1 indicate that two detrital zircon spectra  
170 have a high degree of overlap (Satkoski et al., 2013; Saylor and Sundell, 2016).

171  
172  
173

## 174 2.3 Zircon Optical Profilometry

175 To evaluate the effect of CA on laser ablation excavation rates in zircons, we compared the average depth at  
176 increasing ablation times on a series of laser pits on treated and untreated reference materials. This was accomplished  
177 by generating ten laser ablation pits with excavation times that increased by three seconds (starting at three and  
178 increasing to thirty seconds) in single crystals of treated and untreated grains of zircon reference materials FC1, R33,  
179 and SL. The resulting pits were imaged using a Veeco Wyko NT9800 Optical Profilometer and depth maps, 3-D  
180 images, and crosscut profiles were created using the Vison software produced by Veeco. The images and profiles  
181 allowed for the estimation of pit depths and can be used to calculate excavation rates when combined with the known  
182 ablation periods (Fig. 2). Laser ablation pits were also imaged and measured on three treated and five untreated  
183 unknowns from sample MIGU-02.

184

## 185 2.4 CA-ID-TIMS Zircon U-Pb Geochronology

186 Sample MIGU-02, a granitoid from the Guyana Shield, was analyzed by CA-ID-TIMS at Purdue University  
187 to provide a reference date to compare the chemically abraded and untreated LA-ICP-MS analyses. Following the  
188 chemical abrasion methods described above, individual zircons were spiked with the EARTHTIME  $^{205}\text{Pb}$ - $^{233}\text{U}$ - $^{235}\text{U}$   
189 isotopic tracer (Condon et al., 2015; McLean et al., 2015) and loaded into a Parr acid digestion vessel with 28M HF.  
190 The vessel was then held at 210°C for 60 hours for zircon dissolution. After dissolution, the samples were dried down  
191 and converted to chloride form, by adding 75  $\mu\text{l}$  7M HCl, reassembling the Parr acid digestion vessel, and holding it  
192 at 180°C for 12 hours. After conversion to chloride form, the solution was converted to 3M HCl in preparation for  
193 anion exchange chromatography. Pb and U were purified from these solutions using AG-1x8 anion exchange resin  
194 following procedures modified from Krogh (1973). The resulting aliquots were dried down to a chloride salt before  
195 being dissolved in silica gel, dried onto rhenium filaments, and loaded into an IsotopX Phoenix TIMS for analysis. Pb  
196 isotopic measurements were made by peak hopping on a Daly detector and corrected for mass dependent isotopic  
197 fractionation using an  $\alpha = 0.147 \pm 0.028$  (%amu) and deadtime = 29.9 ns, derived from repeat measurements of the  
198 NBS981 Pb reference material. We assume that all  $^{204}\text{Pb}$  is from laboratory contamination and correct for it using a  
199 laboratory Pb isotopic composition of  $^{206}\text{Pb}/^{204}\text{Pb} = 18.82 \pm 0.74$  ( $2\sigma$ ),  $^{207}\text{Pb}/^{204}\text{Pb} = 15.52 \pm 0.63$  ( $2\sigma$ ),  $^{208}\text{Pb}/^{204}\text{Pb} =$   
200  $37.93 \pm 1.60$  ( $2\sigma$ ) derived from repeat total procedural blank measurements run during 2022. Uranium was run as an  
201 oxide ( $\text{UO}_2$ ) and isotopic measurements were made statically using Faraday detectors and corrected for fractionation  
202 using the known ratio of  $^{233}\text{U}/^{235}\text{U}$  in the EARTHTIME  $^{205}\text{Pb}$ - $^{233}\text{U}$ - $^{235}\text{U}$  isotopic tracer (Condon et al., 2015; McLean  
203 et al., 2015) and assuming a zircon  $^{238}\text{U}/^{235}\text{U}$  value of  $137.818 \pm 0.045$  (Hiess et al., 2012). Data reduction was done  
204 using the ET\_Redux software package (Bowring et al., 2011) and the decay constants of Jaffey et al. (1971). All  
205 isotopic data measured via CA-ID-TIMS are presented in Supplemental Table S17.

206

## 207 3. Results

### 208 3.1 CA-LA-ICP-MS U-Pb Geochronology of Zircon Reference Materials

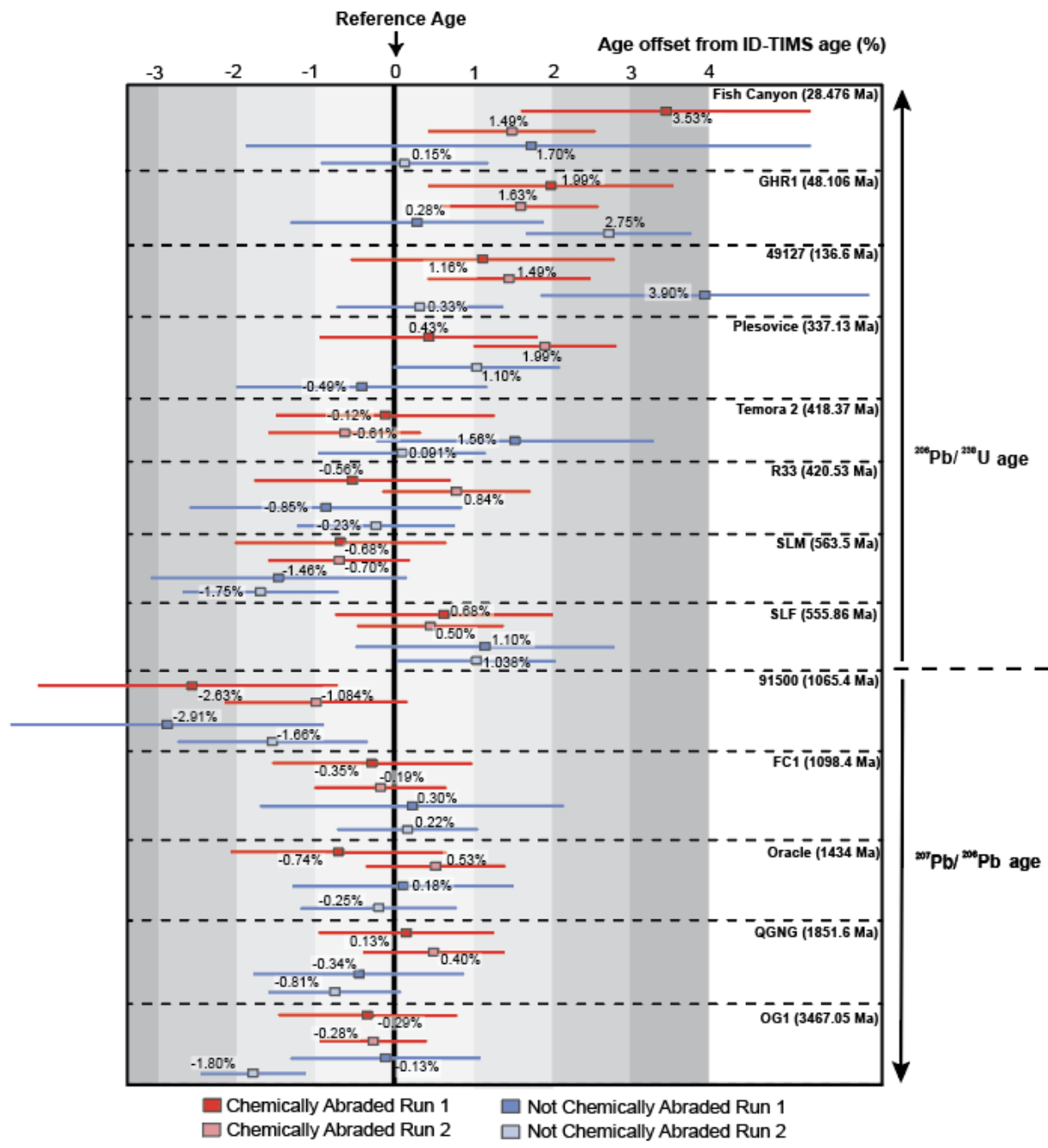
209 Treated and untreated aliquots of thirteen different zircon U-Pb reference materials (Table 1) were analyzed  
210 in this study to further assess whether chemical abrasion systematically biases U-Pb dates. The reference materials  
211 were analyzed during two round-robin runs using the approach described above. The first run targeted 15 zircon grains

212 from treated and untreated aliquot of reference materials. During the second run, 30 zircon grains were targeted.  
213 Because FC1 was used as a primary reference material for calibration of the LA-ICP-MS, approximately 30 FC-1  
214 zircons were analyzed during run one and 87 were analyzed during run two in both treated and untreated aliquots.  
215 This led to 117 FC1 grains analyzed per treated and untreated aliquots of reference material. The total number of  
216 zircons analyzed was 653 in each of the chemically abraded and untreated aliquots of reference materials. Of the 653  
217 grains in the chemically abraded aliquots, 631 analyses (96.6%) were retained following filtering for discordance,  
218 whereas 608 analyses (93.5%) were retained in the untreated aliquot. These results further confirm that CA helps  
219 mitigate Pb-loss and improve the percentage of retained concordant LA-ICP-MS analyses (e.g., Crowley et al., 2014;  
220 von Quadt et al., 2014). The most extreme change in concordance and data retention occurred between treated and  
221 untreated FC-1 zircon (1098.4 Ma). Of the 117 grains analyzed in both the treated and untreated aliquots, 99.1% of  
222 analyses were retained in the chemically abraded aliquot versus 82.2% in the untreated aliquot. Discordance criteria  
223 used for filtering the above data were reverse discordance larger than 5%,  $^{206}\text{Pb}/^{238}\text{U}$  errors larger than 10%, and/or  
224 maximum discordance of over 20%. Overall, the discordant FC1 grains in both runs had low U cps and significantly  
225 older  $^{206}\text{Pb}/^{238}\text{U}$  dates (>1250 Ma; Fig. S15).

226 The weighted mean dates of CA and non-CA reference materials are all within 0.1 – 4% of the reference  
227 ages determined by ID-TIMS (Fig. 1). Therefore, despite an increase in the percent of concordant treated grains  
228 relative to untreated grains, weighted means of acceptable analyses are indistinguishable and indicate that it is unlikely  
229 that chemical abrasion biases U-Pb dates within LA-ICP-MS instrument uncertainty. The greatest scatter in calculated  
230 weighted mean ages (~4 to 0.1% age offset from reference date) is in both the treated and untreated Mesozoic to  
231 Cenozoic reference materials. Scatter is improved by chemical abrasion in Paleozoic reference materials (2 to 0.8%  
232 age offset) and excellent for Proterozoic and Archean aliquots (0.6 to -0.7%). Additionally, concordant analyses of  
233 treated aliquots have overall lower  $^{238}\text{U}$  cps compared to the untreated aliquots (Fig. S15), indicating that chemical  
234 abrasion dissolved zones of high U concentrations where Pb-loss is most likely to have occurred (Widmann et al.,  
235 2019; McKanna et al., 2023). Since reference materials are selected for their homogeneous isotopic compositions, it  
236 is not surprising that there is similarity in dates between treated and untreated aliquots. The reproducibility of U-Pb  
237 dates for all of the reference materials is strong evidence that a single primary reference material (FC-1 in this case)  
238 can be used to correct for instrumental fractionation across a wide range of zircon ages and trace element compositions  
239 for chemically abraded zircon.

240 Despite the overall similarity in bias between treated and untreated reference materials, the behavior of some  
241 reference materials warrants further discussion. The CA-LA-ICP-MS weighted mean  $^{206}\text{Pb}/^{238}\text{U}$  dates for two  
242 Cenozoic reference materials were older than the CA-ID-TIMS reference date. Chemical abrasion of GHR1 zircon  
243 led to an increase of concordant grains, but an older  $^{206}\text{Pb}/^{238}\text{U}$  weighted mean date (Fig. S2). We attribute this  
244 difference to the presence of slightly older xenocrysts within the sample (e.g., Eddy et al., 2019). We see a similar  
245 result for Fish Canyon tuff zircon where the CA aliquot showed increased concordance, but the calculated mean age  
246 was offset more from the reference age than the no-CA aliquot (Fig. S1). This sample contains significant antecrysts  
247 that might bias its results (e.g., Wotzlaw et al., 2013). Indeed, increased precision and accuracy in analyses of young  
248 suites of igneous zircon routinely find overdispersion that can be related to protracted zircon growth or the presence

249 of xenocrysts/antecrysts. Thus, the slight variability in weighted mean dates for GHR1 and Fish Canyon samples in  
 250 CA-LA-ICP-MS analyses is not entirely unexpected and therefore unlikely to reflect of a systematic bias of the CA-  
 251 LA-ICP-MS method. Additionally, the 91500 reference material has shown substantial negative age offset in other  
 252 studies (Gehrels et al., 2008; Schoene et al., 2014), but the origin of these offsets has remained enigmatic, and the  
 253 offset in this study is not surprising.  
 254

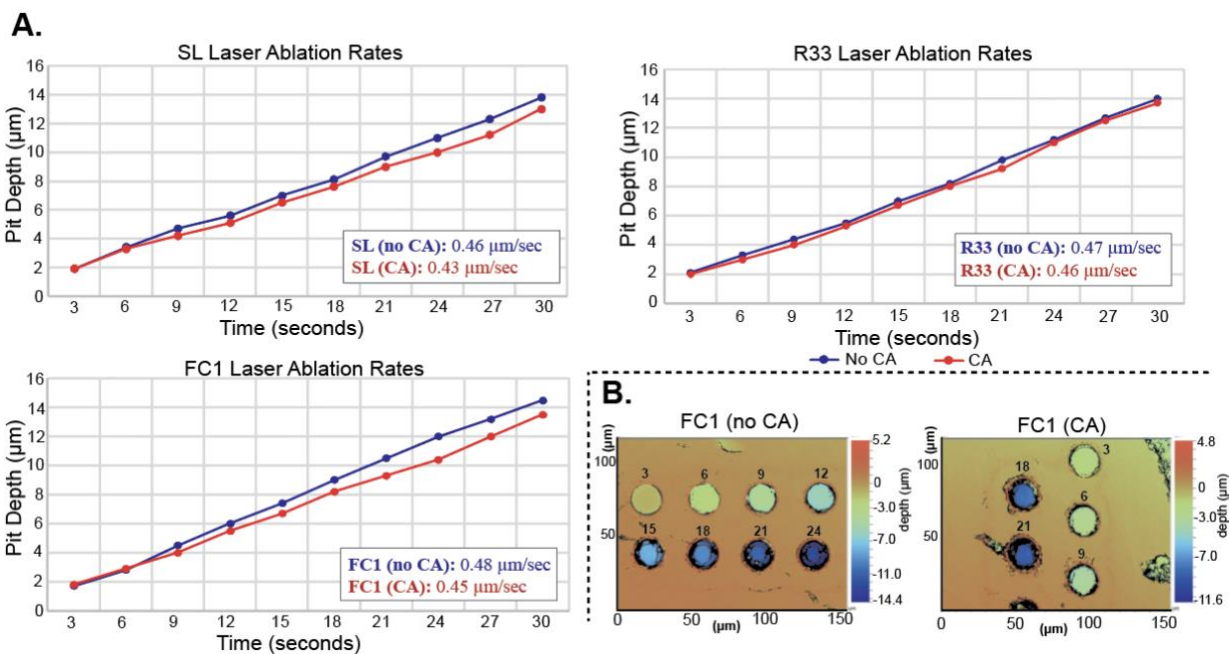


255



256 **Figure 1.** Comparison of  $^{206}\text{Pb}/^{238}\text{U}$  and  $^{207}\text{Pb}/^{206}\text{Pb}$  (CA)-LA-ICP-MS ages with CA-ID-TIMS ages for thirteen  
257 reference materials that range in age from 28 to 3467 Ma. Each square is the weighted mean of a set of (CA)-LA-ICP-  
258 MS measurements shown as the percent offset from the known reference age (ID-TIMS). The uncertainty is reported  
259 as 2-sigma standard error of the weighted mean. Chemical abrasion of treated aliquots was conducted at Purdue  
260 University and laser ablation analyses were conducted at Arizona LaserChron Center on the Thermo Element2 single-  
261 collector ICP-MS. Methods for LA-ICP-MS at LaserChron using the Element2 are described by Pullen et al. (2018).  
262

263 Variations in laser ablation behavior between primary reference materials used for standardization and  
264 samples is a direct result of differences in zircon matrices and are known as ‘matrix effects’ (Marillo-Sialer et al.,  
265 2016). Differences in zircon matrices are related to numerous factors (see review in Marillo-Sialer et al., 2016),  
266 including presence/absence of trace elements (Black et al., 2004), the amount of radiation damage (Allen and  
267 Campbell, 2012), and the degree of crystallinity (Steely et al., 2014). These factors all impact the laser’s ability to  
268 couple with the surface of the zircon, directly impacting laser ablation rates and the rates of down-hole fractionation.  
269 As a result, matrix-effects can lead to systematic shifts in LA-ICP-MS data and may be a contributor in observed shifts  
270 in treated and untreated aliquots of reference materials in this study (Fig. 1). In order to constrain how CA impacts  
271 laser coupling and ablation rates between treated and untreated reference materials, we ablated 10 spots on a single  
272 treated and untreated zircon crystal of FC1, SL, and R33 (n=60; Table S14). For each individual spot 1-10 on a  
273 reference material, we incrementally raised the ablation duration by 3 seconds (i.e., by 21 individual laser pulses at 7  
274 Hz). This resulted in 10 different spots with ablation durations ranging from 3 to 30 seconds (21 to 210 laser pulses)  
275 and allowed us to calculate laser ablation rates for both treated and untreated zircon. Overall, laser ablation rates varied  
276 linearly with time (0.43 to 0.46  $\mu\text{m}/\text{sec}$ ) and were similar for treated and untreated aliquots of all primary reference  
277 materials (Fig. 2). Similar ablation rates were observed across all three different treated and untreated aliquots of  
278 primary reference materials. This suggests 1) the primary reference materials have similar zircon matrix densities and  
279 ablate at similar rates (Marillo-Sialer et al., 2014; 2016), and 2) chemical abrasion does not change the zircon matrix  
280 density or alter the zircon surface of primary reference materials in a way that drastically alters laser coupling or  
281 ablation rates.  
282



284 **Figure 2. A.** Line graphs showing pit depths ( $\mu\text{m}$ ) versus time (seconds) for unabraded and abraded aliquots of primary  
 285 reference materials. Each data point represents an individual pit. Untreated reference materials have slightly deeper  
 286 pit depths and ablate at marginally faster rates, but overall, rates of ablation for treated and untreated reference  
 287 materials are similar. **B.** An example of one of the VEECO surface data maps showing pit depths on treated and  
 288 untreated zircon of FC1. Pits are labeled with the duration in seconds of ablation. See Supplemental Table S14 for all  
 289 pit depth data from abraded and unabraded reference materials.

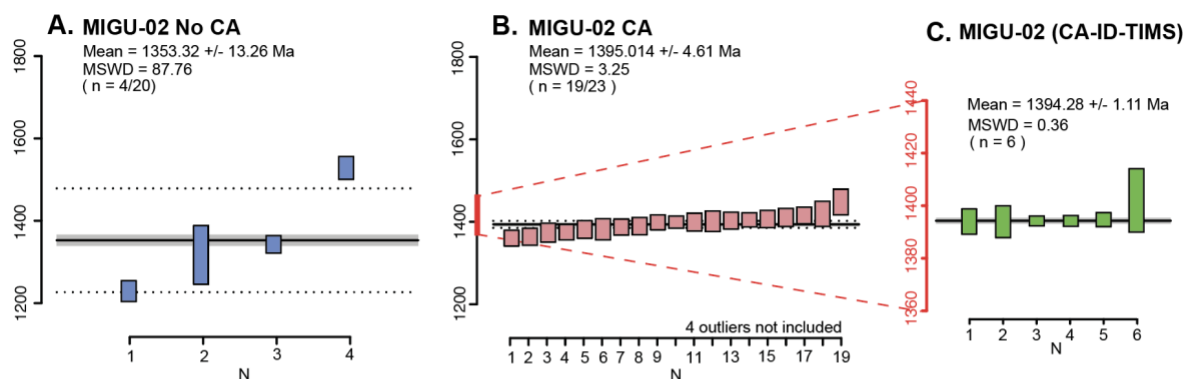
290

### 291 3.2 Untreated and CA- U-Pb Zircon LA-ICP-MS Analyses of Metamict Zircon

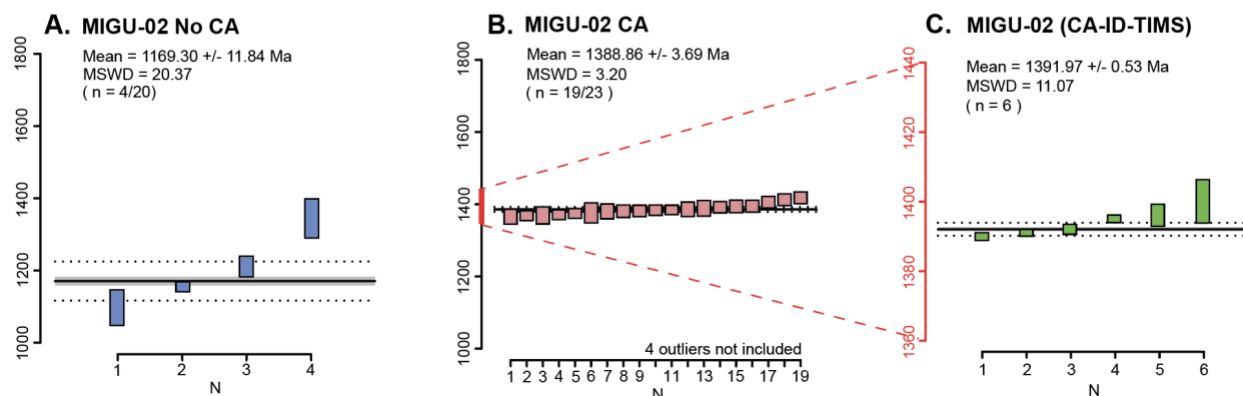
292 A Precambrian granite sample from the Parguaza Complex in the North Guyana Shield (MIGU-02; N 5° 21'  
 293 3.70"; W 67° 41' 33.41") that has experienced substantial radiation damage was analyzed to assess the effects of  
 294 chemical abrasion on grains with significant Pb-loss. Untreated (n = 20) and treated aliquots (n = 23) of MIGU-02  
 295 were analyzed at the ALC and compared to a reference age determined by CA-ID-TIMS (n=6) at Purdue University  
 296 (Fig. 3; Tables S14 and S15). During the bulk chemical abrasion process, 80-85% of MIGU-02 grains fully dissolved,  
 297 leaving only a small fraction of the original aliquot to be used for analyses.

298

### $^{207}\text{Pb}/^{206}\text{Pb}$ Rank Order Plots



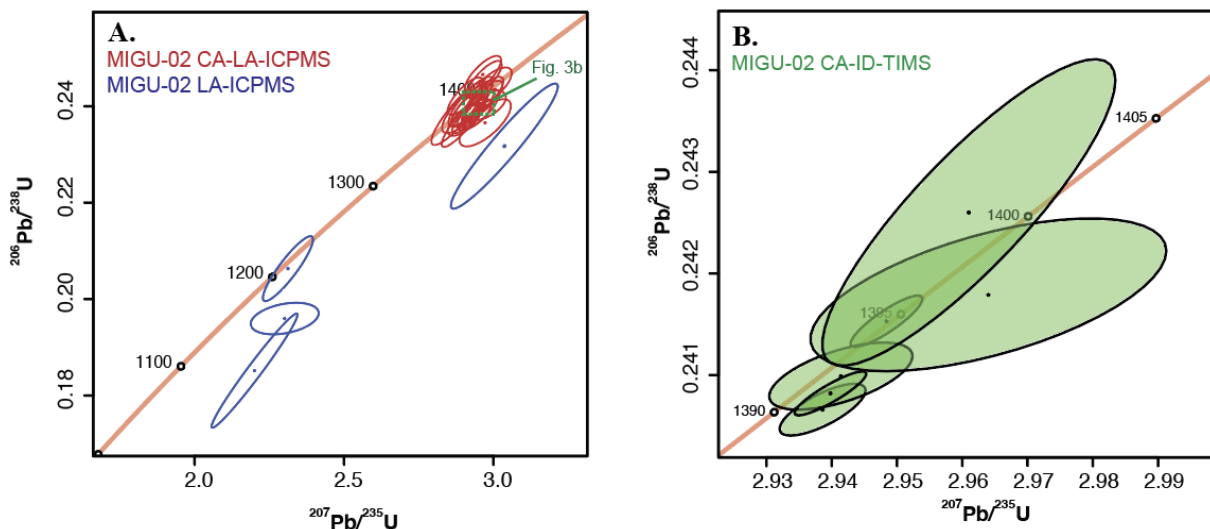
### $^{206}\text{Pb}/^{238}\text{U}$ Rank Order Plots



299 **Figure 3.** Rank order plots of calculated  $^{207}\text{Pb}/^{206}\text{Pb}$  and  $^{206}\text{Pb}/^{238}\text{U}$  ages for treated and untreated MIGU-02 aliquots  
 300 and of the reference age for MIGU-02 obtained using CA-ID-TIMS. **A.** Untreated samples of MIGU-02 show large  
 301 degree of scatter in dates and substantial deviation from the reference age. **B.** Treated zircons show a significant  
 302 increase in precision and accuracy of ages relative to the reference age. **C.** Reference age for MIGU-02 determined  
 303 using the weighted mean of six grains. See text for discordance criteria.

304  
 305 The  $^{207}\text{Pb}/^{206}\text{Pb}$  CA-ID-TIMS reference age for MIGU-02 is 1394.28 +/- 1.11 Ma (n=6, MSWD = 0.36),  
 306 while the  $^{206}\text{Pb}/^{238}\text{U}$  dates are more scattered (Fig. 3). The scatter indicates that U/Pb elemental fractionation occurred  
 307 during chemical abrasion in one analysis (slight reverse discordance) and residual Pb-loss remained in others (normal  
 308 discordance)(Fig. 4). Nevertheless, a weighted mean date of the  $^{206}\text{Pb}/^{238}\text{U}$  CA-ID-TIMS dates is 1391.97 +/- 0.53 Ma  
 309 (n = 6, MSWD = 11.06) and indicates that residual Pb-loss only affects the dates at the <0.5% level. Untreated LA-  
 310 ICP-MS analyses of MIGU-02 show significant discordance (Fig. 4) and only 4 analyses (n=4/20; 80% discordant)  
 311 were retained after filtering by AgeCalcML v.1.42. Chemical abrasion substantially increased the number of  
 312 concordant analyses (n = 23/23). Fifteen analyses were removed from the untreated aliquot dataset and seven analyses  
 313 were removed from the treated aliquot dataset because they hit epoxy and are not included in the totals. Although all  
 314 grains were concordant in the treated aliquot, four grains were not included in the weighted mean because they had a  
 315 significantly older  $^{207}\text{Pb}/^{206}\text{Pb}$  dates (1571-1900 Ma) than the CA-ID-TIMS reference date (Table S14) and are likely

316 xenocrystic. The weighted mean  $^{207}\text{Pb}/^{206}\text{Pb}$  date from the untreated MIGU-02 aliquot is 1353.32 +/- 13.26 Ma (n =  
 317 4/20; MSWD = 87.76) and the treated aliquot is 1395.014 +/- 4.61 Ma (n = 19/23; MSWD = 3.25). The mean  $^{206}\text{Pb}/^{238}\text{U}$   
 318 date of the untreated aliquot is 1169.30 +/- 11.84 Ma (MSWD = 20.37) and the mean  $^{206}\text{Pb}/^{238}\text{U}$  date of the treated  
 319 aliquot is 1388.86 +/- 3.69 Ma (MSWD = 3.20). Thus, the dates from treated zircon show a significant increase in  
 320 concordance, precision, and accuracy relative to the reference date as determined by CA-ID-TIMS (Fig. 3).  
 321



322  
 323 **Figure 4. A.** Untreated and treated aliquots of MIGU-02 shown on a concordia plot. Non-CA MIGU-02 dates are  
 324 discordant whereas CA dates fall on concordia and overlap the reference age. **B.** All CA-ID-TIMS analyses of MIGU-  
 325 02 shown on a concordia plot. One date shows slight reverse discordance whereas all other dates fall on concordia or  
 326 have slight normal discordance.

327  
 328 All the CA-treated analyses have lower  $^{238}\text{U}$  beam intensity than the untreated grains suggesting that CA  
 329 selectively removed zones of higher U concentration (Fig. 5). Furthermore, the untreated zircon with the highest  $^{238}\text{U}$   
 330 beam intensity are associated with U-Pb dates that are  $>\pm 20\%$  discordant (Table S16). Since uranium concentration  
 331 is correlated to radiation damage in old zircon, this result reinforces the observation that CA is an effective tool for  
 332 removing damaged zones of the zircon (Nasdala et al., 2005; Widmann et al., 2019). Pit depths were measured on five  
 333 untreated and three treated zircons from MIGU-02 (Table S15). The average pit depth for untreated grains of MIGU-  
 334 02 is  $\sim 10.34 \mu\text{m}$ , whereas it is  $\sim 8.1 \mu\text{m}$  for the treated aliquot. This indicates that the pit depths of the untreated aliquot  
 335 of MIGU-02 are  $\sim 25\%$  deeper than the treated aliquot and that CA does have an impact on the laser ablation rate in  
 336 highly metamict samples.

337 We acknowledge that for samples with significant radiation damage, there is always the possibility that the  
 338 entire sample will dissolve during chemical abrasion, and it is up to the researcher to determine if this technique is  
 339 appropriate for their objectives. Running a high-n data acquisition on highly damaged zircon might ultimately yield  
 340 enough concordant analyses to make a confident age determination, but analyses of MIGU-02 that passed typical  
 341 discordance filters were inaccurate by up to  $-11\%$  for the  $^{207}\text{Pb}/^{206}\text{Pb}$  dates and  $-21\%$  for the  $^{206}\text{Pb}/^{238}\text{U}$  dates (Fig. 3),

342 suggesting that even filtered data may be inaccurate for metamict zircon. In contrast, the chemically abraded aliquot  
343 did not have these issues, despite the significant loss of zircon grains during the HF chemical attack.  
344

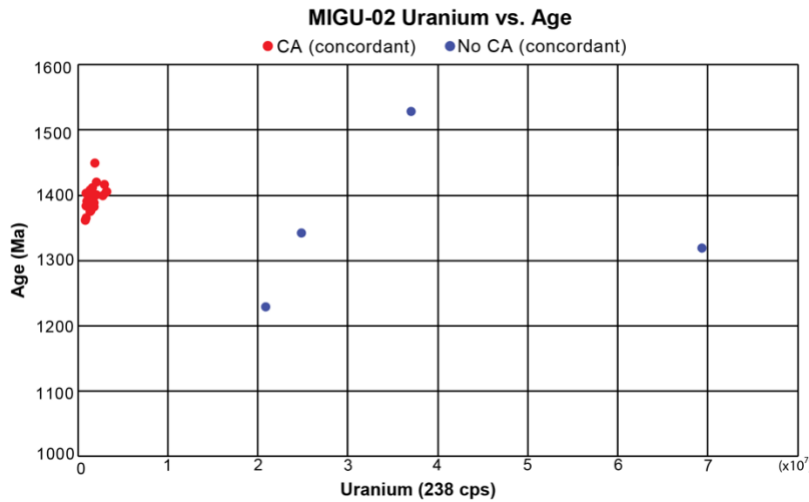


**Figure 5.** Uranium (238 cps) plotted against  $^{207}\text{Pb}/^{206}\text{Pb}$  age (Ma) for both treated and untreated aliquots of MIGU-02. Only concordant analyses are shown because discordant analyses for MIGU-02 have extremely low  $^{238}\text{U}$  cps. Uranium concentration is directly proportional with radiation damage in zircon with the same low-temperature

357 cooling history. The restricted range of low  $^{238}\text{U}$  cps in the CA-treated grains suggests that CA was effective at  
358 dissolving high U zircon that was more likely to have Pb-loss.

### 359 360 **3.3 Untreated and CA- U-Pb Zircon LA-ICP-MS Analyses of Detrital Zircon**

361 One Phanerozoic (NM8A) and one Precambrian sample (Rora Med) were analyzed to determine how detrital  
362 zircon age distributions compare between chemically abraded and untreated aliquots. We followed the ‘Large-n’  
363 approach of Pullen et al. (2014) for both treated and untreated aliquots to obtain a more robust distribution of ages,  
364 their modes, peak widths, and abundances. For NM8A, we analyzed 512 individual zircons in the treated aliquot and  
365 896 zircons in the untreated aliquot. In Rora Med, we analyzed 1035 zircons in the treated aliquot and 920 zircons in  
366 the untreated aliquot. We used Saylor and Sundell (2016) DZstats program to complete a quantitative assessment of  
367 the similarity between treated and untreated aliquots (See definitions described above; Table S22). Additionally, we  
368 calculated the fraction of grains that defined distinct peak age populations in each aliquot to assess how the proportion  
369 of each population changed after chemical abrasion. Our results show that chemical abrasion (CA) changed the number  
370 and distribution of apparent peak age populations in both DZ samples compared to the non-CA age spectra (Figs. 6  
371 and 7). Most notably, the Phanerozoic age peaks in sample NM8A narrowed, became more defined, and, in some  
372 cases, shifted to slightly older dates.

373

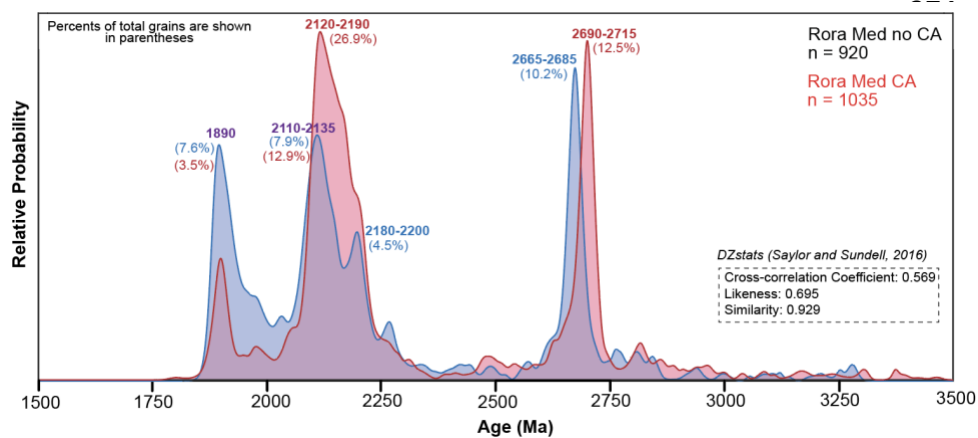


**Figure 6.** Comparison of U-Pb detrital zircon age spectra of not chemically abraded (blue) and chemically abraded (red) aliquots of Rora Med. Areas where age spectra overlap are shaded in purple. Quantitative

384 comparisons of treated and untreated aliquots were completed using Saylor and Sundell (2016) DZstats to calculate  
 385 cross-correlation, likeness, and similarity values. All quantitative comparison analytics are reported in Table S20. The  
 386 percentages above the peaks represent the percentage the peak age population represents out of the total grains. We  
 387 aimed for n=1000 for each aliquot because Pullen et al (2014) shows the distribution of analyzed zircon ages is thought  
 388 to approach the ‘true’ age distribution of the sample.

389  
 390

391 In the Precambrian sample (Rora Med), there are subtle changes in the DZ age spectra between the treated  
 392 and untreated aliquots. Overall, the CA treated aliquot shows a higher percentage of concordant grains (Fig. 6)  
 393 narrower, better defined, peak age populations, changes in the number of peaks present, and a slight but noticeable  
 394 shift in peak age populations to older ages (Fig. 6). Of note, the 1890 Ma peak narrows in the treated aliquot compared  
 395 to the broad peak that covers a range of ages between 1890 and 2000 Ma in the untreated aliquot. However, the fraction  
 396 of grains within this population decreased from 7.6% to 3.5% between the untreated and treated fractions, respectively.  
 397 There is also a change in the shape and number of peaks between the two fractions between 2100 and 2300 Ma. In the  
 398 untreated aliquot, there are three distinct peak age populations (~2120 (~7.9%), 2190 (~4.5%), & 2260 Ma (<2%)),  
 399 whereas in the treated aliquot, there is only one broad peak age population that spans between ~2120-2190 Ma (~30%).  
 400 There is also a distinct shift in the untreated aliquot 2675 Ma peak age population to fifteen million years older in the  
 401 treated aliquot (Fig. 6). Quantitative comparisons support these observations. A likeness coefficient of 0.695 and  
 402 cross-correlation coefficient of 0.569 support there are significant differences in the number, shape, and magnitude of  
 403 certain peak age populations. However, a similarity value of 0.929 indicates that even with these changes for specific  
 404 age populations, there is an overall high degree of overlap in the number and proportion of modes in the detrital zircon  
 405 spectra between treated and untreated aliquots.

406  
 407

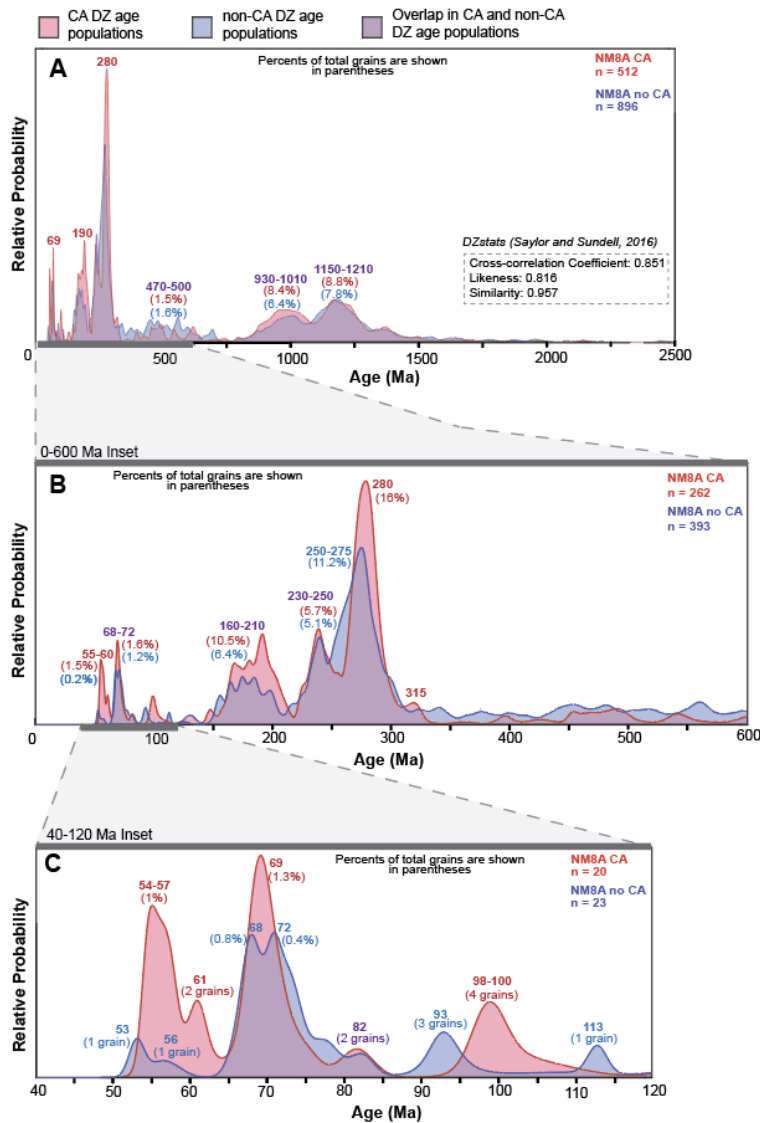


**Figure 7.** Comparison of U-Pb detrital age spectra of not chemically abraded (blue) and chemically abraded (red) aliquots of NM8A. Areas where age spectra overlap are shaded in purple. Quantitative comparisons of treated and untreated aliquots were completed using Saylor and Sundell (2016) DZStats to calculate cross-correlation, likeness, and similarity values. All quantitative comparison analytics are reported in Table S20. The percentages above the peaks represent the percentage the peak age population represents out of the total grains. We aimed for n=1000 for each aliquot as the distribution of analyzed zircons ages is thought to approach the ‘true’ age distribution of the sample (Pullen et al., 2014). Insets A-C show variations of the scale on the x-axis.

433

434 There are also subtle changes in the number of peaks and peak shapes between the treated and untreated  
 435 aliquots of NM8A. The most significant changes observed are increased resolution and definition of Phanerozoic peak  
 436 age populations in the treated aliquot (Fig. 7). For example, between 200-300 Ma, two broad peaks in the untreated  
 437 aliquot sharpen and narrow to two well-defined peak age populations in the treated aliquot (Fig. 7b). Additionally, a  
 438 distinct 190 Ma peak is present in the treated aliquot compared to a broad range of populations between 160 and 210  
 439 Ma in the untreated aliquot. We also see a zone of two broadly defined peaks at 68 and 72 Ma in the untreated aliquot  
 440 sharpen to a singular peak at 69 Ma in the treated aliquot. In the untreated aliquot, the 68-72 Ma age populations make  
 441 up ~1.2% of the total grains in the untreated aliquot, whereas in the treated aliquot the 69 Ma peak age population  
 442 represents ~1.3% of total grains. There is also an older shift from the 93 Ma peak in the untreated aliquot to ~98 Ma  
 443 in the treated aliquot. However, due to the low number of grains within these peak age populations, it is possible these  
 444 shifts are related to subtle differences between the two fractions and not a consequence of the chemical abrasion

445 process. For example, the peak height change in the 93 Ma population (3 grains; untreated aliquot) to the 98-100 Ma  
 446 (4 grains; treated aliquot) represents the addition of a single grain (Fig. 7c). Other shifts and changes in peak age  
 447 populations that are <120 Ma (Fig. 7c) cannot be confidently constrained due to the low number of analyses that define  
 448 those populations (1-2 grains). The fraction of concordant grains is indistinguishable between treated and untreated  
 449 aliquots of NM8A (Fig. 8). Quantitative comparisons of treated and untreated aliquots further support these results  
 450 and similarity, cross-correlation, and likeness values are all >0.8 (Fig. 6). The Similarity value of 0.957 indicates a  
 451 strong overlap in the number and proportion of detrital zircon peak age populations overall. Slightly lower, but still  
 452 high, cross-correlation (0.851) and likeness (0.816) coefficients support minor shifts in the number of peak age  
 453 populations (modes) and changes in peak heights (magnitude).

454  
 455

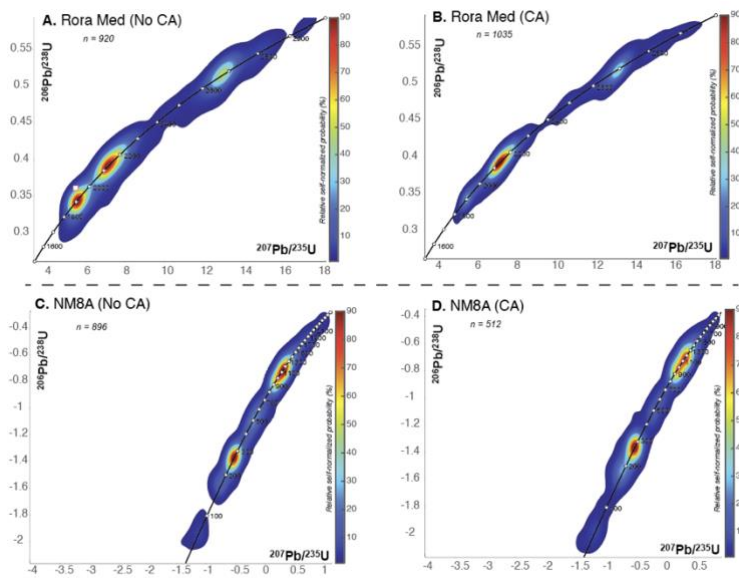


**Figure 8.** Density contour concordia diagrams for not chemically abraded and chemically abraded aliquots of detrital zircon samples NM8A and Rora Med (A-D). There is substantial improvement in the scatter of concordant analyses in the chemically abraded aliquot of the Proterozoic Rora Med sample compared to the untreated aliquot (A-B). However, both aliquots of the Phanerozoic NM8A sample are indistinguishable (C-D). Please note that the concordia diagrams for NM8A (C-D) are plotted on a logarithmic scale to best display

469 the large range Phanerozoic to Precambrian ages.

470  
 471 **4. Discussion**

472 Our study shows that chemical abrasion prior to LA-ICP-MS analysis does not negatively affect resulting U-  
 473 Pb dates provided chemically abraded reference materials are used as the primary reference material for calibration  
 474 (e.g., Crowley et al., 2014; von Quadt et al., 2014). We also show that chemical abrasion is extremely effective in  
 475 mitigating the effects of Pb-loss in LA-ICP-MS U-Pb dating of zircon that has experienced substantial radiation  
 476 damage. Significant improvement was observed in both  $^{206}\text{Pb}/^{238}\text{U}$  and  $^{207}\text{Pb}/^{206}\text{Pb}$  dates of MIGU-02 zircon relative  
 477 to ID-TIMS results, and also the efficiency of the analyses was dramatically improved by focusing LA-ICP-MS  
 478 analyses on only those grains/fragments that survived the chemical abrasion process and had not sustained significant  
 479 radiation damage. These results reinforce the observations of previous studies that used this approach (Crowley et al.,  
 480 2014; von Quadt et al., 2014) and suggested that the CA-LA-ICP-MS method can be valuable for studies that need  
 481 increased precision and accuracy in LA-ICP-MS U-Pb zircon analyses. Although, care must be taken to ensure data  
 482 is not biased when this pre-treatment is applied.



483 One important consideration is whether chemical abrasion negatively affects the laser ablation process.  
484 Variations in laser ablation pit depths have been directly correlated to the density of the zircon matrix (Marillo-Sialer  
485 et al., 2014; 2016) and changes in ablation rate change down-hole fractionation. Previous research has indicated that  
486 annealing leads to lower ablation rates compared to unannealed zircon and more homogenous rates across annealed  
487 zircon with variable initial degrees of radiation damage (Marillo-Sialer et al., 2016). These observations support results  
488 from Campbell and Allen (2012) that thermal annealing zircon samples prior to LA-ICP-MS will reduce matrix-related  
489 bias and improve accuracy and precision. However, the impact of CA on laser coupling and ablation rates is not as  
490 well characterized. Crowley et al. (2014) found that treated zircons had pit depths that were 25% shallower than  
491 untreated aliquots of zircons that experienced extensive Pb-loss. This is identical to the results for the metamict MIGU-  
492 02 sample in this study in which chemically abraded zircon also had ~25% shallower ablation pits than untreated  
493 zircon (Table S15). The shallower pit depths could be driven by less effective laser coupling in treated aliquots due to  
494 small-scale etching and creation of a 3-D porous texture by partial dissolution (Crowley et al., 2014). In comparison,  
495 laser ablation rates and pit depths in treated and untreated aliquots of primary reference materials were nearly identical  
496 (Fig. 2). This supports conclusions drawn by Crowley et al. (2014) that the extent to which zircon is impacted by CA  
497 is dependent on U concentration and the presence of physical defects and highlights the importance of incorporating  
498 a wide range chemically abraded reference materials in each analytical session.

499 Our data, and the data of Crowley et al. (2014) and von Quadt et al. (2014), indicate that provided care is  
500 taken to use chemically abraded reference materials, the pre-treatment will mitigate Pb-loss and lead to increased  
501 accuracy in LA-ICP-MS U-Pb zircon analyses. Given this apparent benefit, it is natural to extend the technique to  
502 detrital zircon and test the advantages and disadvantages afforded by this method. Crowley et al. (2014) first used this  
503 approach on an Archean graywacke and showed that it did not significantly bias their results. However, this technique  
504 has not been widely used over the last decade. We report similar results to previous studies in that chemical abrasion  
505 does not significantly bias results or negatively affect LA-ICP-MS dates. This is supported by quantitative comparison  
506 tests of the treated and untreated aliquots of both detrital zircon samples that show high degrees of similarity between  
507 aliquots. Minor changes in cross-correlation and likeness values are a result of minor changes in the number of and  
508 magnitude of specific peak age populations between treated and untreated aliquots (Fig. 6 and 7). Our results indicate  
509 that a chemical abrasion pre-treatment may help resolve finer scale features in detrital zircon spectra from the Cenozoic  
510 to the Archean. We attribute this increased resolution mainly to the mitigation of Pb-loss leading to increased accuracy  
511 of the resulting LA-ICP-MS U-Pb dates.

512 The mitigation of Pb-loss is most clearly observed in the sharpening of Neoproterozoic through Cenozoic  
513 age populations because  $^{206}\text{Pb}/^{238}\text{U}$  dates provide the most precise estimate for zircon crystallization in this age range.  
514 Pb-loss can significantly affect the accuracy of dates in this age range since Pb-loss trajectories closely follow  
515 concordia and can result in dates that have apparent concordance despite being inaccurate. These effects can be seen  
516 most clearly in sample NM8A where age peaks narrowed and became more defined (e.g., 250-300 Ma peak age  
517 populations) following chemical abrasion and some peak age populations shifted to slightly older dates (Fig. 7).  
518 Assuming that the zircons that form these populations cooled below the temperature at which radiation damage is  
519 effectively annealed at a similar time, then U content can be used as a proxy for radiation damage (Nasdala et al.,

520 2005; Widmann et al., 2019; McKanna et al., 2023). This is clearly observed for the treated and untreated aliquots of  
521 igneous sample MIGU-02, where the treated aliquot has substantially lower  $^{238}\text{U}$  beam intensities and increased  
522 concordance and accuracy in  $^{206}\text{Pb}/^{238}\text{U}$  dates (Figs. 3, 4, and 5). However, the thermal history is not known *a priori*  
523 for detrital zircon datasets, meaning this same assessment applied to NM8A and Rora Med is more uncertain.

524 To examine whether the reduced Pb-loss we observed in the chemically abraded aliquot reflects the selective  
525 dissolution of zircon with radiation damage, we compared zircon  $^{238}\text{U}$  beam intensity from a particular age range (250-  
526 320 Ma) in NM8A as a first-order approximation (Fig. 9). We assume that the populations in this range likely have  
527 the same low-T history, although this assumption cannot be tested with our data. We also note that these populations  
528 showed the most significant sharpening following chemical abrasion (Fig. 7B). Figure 9 shows that the average  $^{238}\text{U}$   
529 beam intensity of treated grains in this age range is similar, but there is a distinct proportion of treated grains that have  
530 lower  $^{238}\text{U}$  intensities. This supports our interpretation that CA is likely mitigating Pb-loss by dissolving zircon with  
531 high U concentrations and that this process can be observed by the changes in the number of peaks, their shape, and  
532 their magnitude between treated and untreated aliquots. These changes are especially apparent when comparing the  
533 shift and change in magnitude of the Rora Med 2665-2685 Ma (untreated aliquot) peak age to 2690-2715 Ma (treated  
534 aliquot).

535

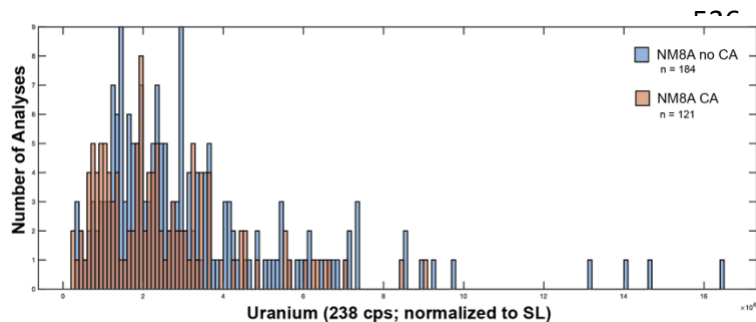


**Figure 9.** Histogram showing  $^{238}\text{U}$  cps (normalized to SL) for zircons in the peak age population between 250-320 Ma in detrital zircon sample NM8A. On the detrital zircon spectra, this age population narrows from one broad peak in the untreated aliquot to a well-defined, narrow

543 peak in the treated aliquot (Fig. 7b). Measured  $^{238}\text{U}$  cps from this peak age population of treated and untreated aliquots  
544 are overall similar, but there is a distinguishable proportion of grains in the treated aliquot that have lower  $^{238}\text{U}$  cps.

545

546 Reduced Pb-loss in Mesoproterozoic and older zircon also benefits detrital zircon studies because ancient  
547 Pb-loss can bias  $^{207}\text{Pb}/^{206}\text{Pb}$  dates of moderately discordant or even (analytically) concordant zircon toward  
548 erroneously young values (Nemchin and Cawood, 2005). This effect has led many laboratories to filter for discordance  
549 within their datasets. Thus, improving concordance will increase the proportion of dates that can be retained in a  
550 detrital zircon study and improve confidence in the identification of peak age populations. One potential issue with  
551 this approach is the possibility that entire zircon populations could be removed during chemical abrasion if they have  
552 high degrees of radiation damage. Surprisingly, we did not see this effect in either NM8A nor Rora Med. This result  
553 is surprising and may be sample specific, since Rora Med zircon from all age populations have low  $^{238}\text{U}$  beam  
554 intensities (Fig. 10b). Although our RoraMed sample did not entirely lose any age populations during CA, changes in  
555 the magnitude of peak heights suggests preferential dissolution of some age populations associated with Pb-loss. This  
556 feature may be unique to Precambrian samples with overall low zircon U concentrations and/or recent exhumation of

557 the sedimentary rocks to the temperature conditions where radiation damage can accumulate and Pb-loss occurs.  
 558 Regardless, both NM8A and Rora Med have similarity values of >0.9 (Figs. 6 and &), indicating that similar peak age  
 559 populations and proportions are present in both treated and untreated aliquots. Therefore, it is unlikely that chemical  
 560 abrasion would impact detrital zircon spectra in a way that would make aliquots look as though they were sampling  
 561 different source terranes.  
 562

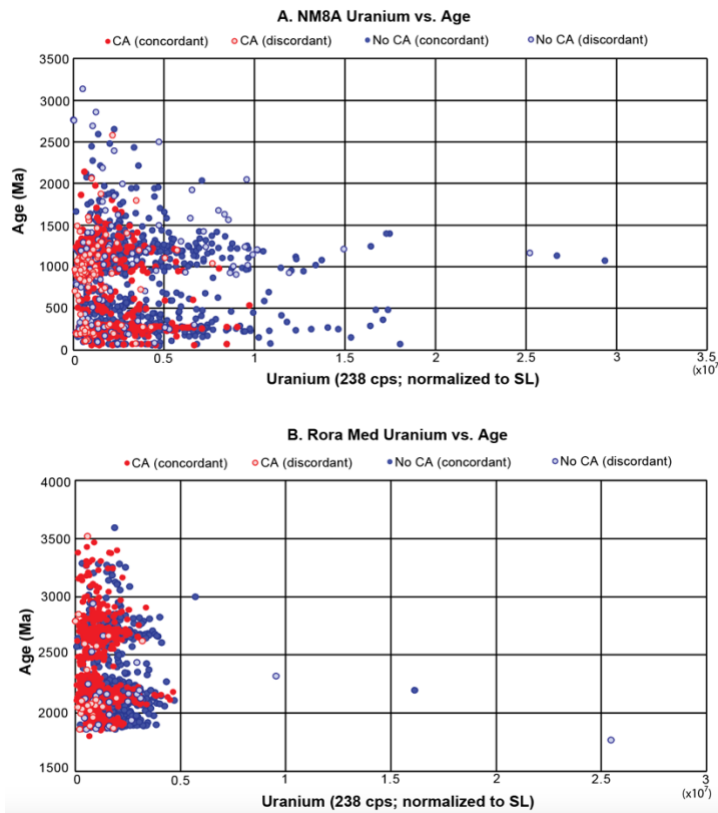


**Figure 10.** Scatter plot of  $^{238}\text{U}$  cps (normalized to SL) plotted against the age (Ma) for both treated and untreated aliquots of **A. NM8A** and **B. Rora Med**. Both concordant and discordant analyses are shown. Overall, CA appears effectively reduce scatter in  $^{238}\text{U}$  cps in all age populations compared to the untreated aliquot, but most significantly reduces scatter in Precambrian ages.

581  
 582 The nature of sediment transport may also work to remove metamict zircon prior to deposition in certain  
 583 environments. Hydraulic sorting, mechanical abrasion, and weathering, can naturally bias detrital zircon populations  
 584 present in a different lithologies (Malusa et al., 2013; Ibañez-Mejía et al., 2018). For example, Ewing et al. (2003)  
 585 noted that metamictization leads to structural damage of the zircon crystal structure and that this can be correlated to  
 586 a decrease in density and hardness. These changes lead metamict zircon to be more prone to destruction during river  
 587 transport (Fedó et al., 2003; Hay and Dempster, 2009a). In particular, Hay and Dempster (2009a) argue that inclusion-  
 588 rich and metamict zircon are broken during sediment transport, and that these fragments do not survive being  
 589 incorporated into clastic sandstone deposits. Instead, these smaller fragments can be swept out to more distal  
 590 depositional environments. Small zircon are also typically lost during sample preparation (Hietpas et al., 2011; Slama  
 591 and Kosler, 2012), meaning that both natural and laboratory processes may preferentially lead to a high proportion of  
 592 undamaged zircon in sandstone samples. Thus, while we did not observe the removal of specific age populations  
 593 following chemical abrasion in the two detrital zircon samples that were analyzed in this study, and there are reasons

594 to suspect that natural and laboratory processes will favor the analysis of undamaged zircon anyway, we recognize  
595 that other samples may behave differently. Future users of this technique should carefully consider this possibility in  
596 their datasets.

597 Another potential benefit of chemical abrasion is the preferential dissolution of inclusions within zircon  
598 during the partial dissolution step (McKanna et al., 2023). Inclusions harbor  $Pb_c$  that can be incorporated into the  
599 analyzed volume during laser ablation, reducing the  $Pb^*/Pb_c$  and limiting measurement precision and accuracy. When  
600 comparing the  $Pb^*/Pb_c$  ratios of treated and untreated aliquots of MIGU-02, we see a clear distinction that treated  
601 zircons have a much higher  $Pb^*/Pb_c$  ratio for similar ranges in  $^{238}U$  beam intensity (Fig. 11). We note that the overall  
602  $^{238}U$  beam intensities for the treated aliquot of MIGU-02 are low compared to the untreated aliquot, as we have already  
603 shown that CA for metamict zircon effectively removes high-U zones where Pb-loss is most likely to have occurred  
604 (see above discussion; Fig. 5). Regardless, the increased  $Pb^*/Pb_c$  ratio for the treated aliquot of MIGU-02 shows that  
605 this method is also efficient in removing inclusions with high  $Pb_c$  content and/or highly damaged domains where  $Pb_c$   
606 might have been introduced by fluids. These two effects are correlated with an increased fraction of concordant grains  
607 and increased precision and accuracy in  $^{206}Pb/^{238}U$  zircon dates in the chemically abraded aliquot. These observations  
608 support the benefits of utilizing CA prior to LA-ICP-MS measurements in metamict igneous zircon suites. A  
609 comparison of the  $Pb^*/Pb_c$  ratios in treated and untreated aliquots of detrital samples (Fig. S18) shows similar behavior  
610 in Rora Med with slightly higher  $Pb^*/Pb_c$  in the treated aliquot and no change in the  $Pb^*/Pb_c$  ratios in NM8A. We  
611 conclude that it is likely that CA is removing inclusions prior to analysis of detrital zircons as well. However, it is  
612 difficult to isolate this effect since detrital zircons are sourced from various terranes and we cannot confidently  
613 compare the  $Pb^*/Pb_c$  of zircon with the same age, U concentration, and thermal history.

614

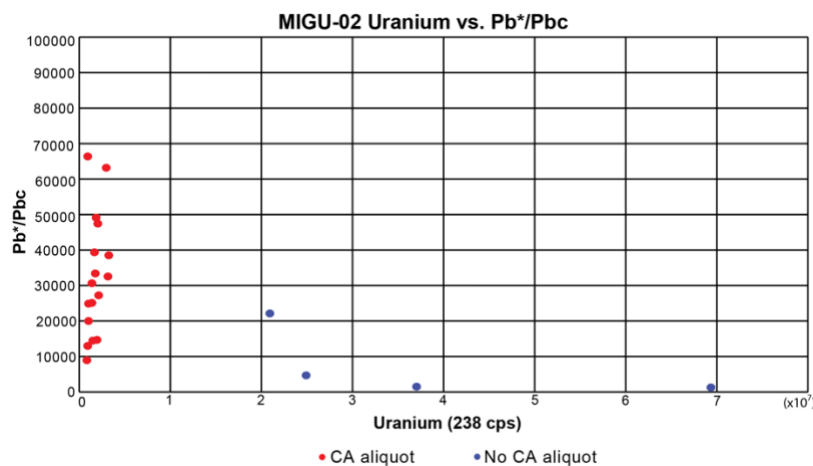


**Figure 11.**  $Pb^*/Pb_c$  ratios are plotted against  $^{238}U$  cps for MIGU-02. The  $Pb^*/Pb_c$  ratios in the treated aliquot of MIGU-02 are significantly higher than the untreated aliquot for similar concentrations of U. Higher  $Pb^*/Pb_c$  ratios in the treated aliquot of MIGU-02 can be attributed to reduction of  $Pb_c$  by removal of inclusions.

625

626

## 627 6. Conclusions and Recommended Applications

628 Chemical abrasion is a widely used tool in the zircon U-Pb ID-TIMS community (*see reviews in* Schoene,  
629 2014; Schaltegger et al., 2015), where it has been repeatedly shown to mitigate the negative effects on age accuracy  
630 introduced by Pb-loss (Mundil et al., 2004; Mattinson, 2005; Widmann et al., 2019). Recent efforts to extend chemical  
631 abrasion to LA-ICP-MS analyses have also shown that this pre-treatment can be beneficial (Crowley et al., 2014; Von

632 Quadt et al., 2014; McKanna et al., 2023; Sharman and Malkowski, 2023). The extension of this pre-treatment to  
633 large-n detrital zircon analyses is a natural outgrowth of these efforts. Our results indicate no negative effects from  
634 chemical abrasion prior to LA-ICP-MS analyses and that the technique results in improved percentages of concordant  
635 grains, reduced uncertainty, and, at least for the highly radiation damaged igneous sample we studied here, accuracy  
636 of measured U-Pb dates. For DZ samples, these benefits appear to translate to more defined and slightly older  
637  $^{206}\text{Pb}/^{238}\text{U}$  age peaks for Phanerozoic zircon, and more concordant analyses, and in some cases slightly older  
638  $^{207}\text{Pb}/^{206}\text{Pb}$  dates for Precambrian zircon. One potential drawback of this pre-treatment is the possibility that age  
639 populations characterized by high-U zircon may be selectively dissolved during chemical abrasion. We did not observe  
640 this effect in either of our tested samples. However, we remain wary of its possibility in other samples with highly  
641 damaged Precambrian zircon populations, and so future practitioners are advised caution. The differences between  
642 age distributions in our analyzed detrital zircon spectra are slight and indicate that the Pb-loss present in typical  
643 untreated analyses would not significantly alter the interpretation of sediment source terranes at a broad scale.  
644 However, chemical abrasion did sharpen several Phanerozoic peak ages and led to an increased percentage of  
645 concordant grains in Precambrian zircon populations. This indicates that the pre-treatment may be useful in certain  
646 scenarios in which researchers may require increased resolution of detrital zircon age spectra to distinguish fine-scale  
647 variations in provenance, sediment source terranes, or source characteristics. Ongoing research aims to test this  
648 method's impact on improving the precision and accuracy of maximum depositional age (MDA) estimations.

649

#### 650 **Supplement**

651 All datasets utilized in this study are available in the Supplementary Material online at:

652

#### 653 **Author contribution**

654 EED, MPE, and MIM all helped design experiments for treated and untreated zircon aliquots and EED prepared all  
655 bulk chemically abraded aliquots and conducted CA-ID-TIMS experiments. FM and EED both conducted LA-ICP-  
656 MS and CA-LA-ICP-MS experiments. FM and MIM designed and FM conducted zircon optical profilometry  
657 experiments. All authors participated in the interpretation and discussion of results. EED prepared the figures and  
658 manuscript.

659

#### 660 **Competing Interests**

661 The authors declare no competing interests.

662

#### 663 **Acknowledgments**

664 We thank the Arizona LaserChron Center (ALC) for sharing samples and reference materials and for helping  
665 analyze these samples. Specifically, we thank G. Gehrels, M. Pecha, D. Alberts, W. Allen, M. Foley, and T. Milster.  
666 We also thank R. Ickert for help designing a system for bulk CA at Purdue. All LA-ICPMS measurements were  
667 made at the Arizona LaserChron Center under NSF-EAR 2050246 for support of the Arizona LaserChron Center  
668 and all CA steps and CA-ID-TIMS measurements were completed at Purdue University's Radiogenic Isotope  
669 Geology Lab (RIGL) under NSF-EAR-2151277 to M. Eddy.

670

671 **References**

- 672 Anderson, T.: Detrital zircons as tracers of sedimentary provenance: limiting conditions from statistics and  
673 numerical simulation, *Chemical Geology*, 216, 249–270, doi: <https://doi.org/10.1016/j.chemgeo.2004.11.013>, 2005.
- 674
- 675 Balan, E., Neuville, D.R., Trocellier, P., Fritsch, E., Muller, J. P., Calas, G.: Metamictization and chemical durability  
676 of detrital zircon, *Am. Mineral.*, 86, 1025-1033, 2001.
- 677
- 678 Bateman, H.: Solution of a system of differential equations occurring in the theory of radioactive transformations,  
679 *Proceedings of the Cambridge Philosophical Society*, 15, 423-427, 1910.
- 680
- 681 Black, L.P.: Recent Pb loss in zircon: a natural or laboratory-induced phenomenon?, *Chemical Geology*, 65 25-33,  
682 1987.
- 683
- 684 Black, L.P., Kamo, S.L., Allen, C.M., Aleinikoff, J.N., Davis, D.W., Korsch, R.J., and Foudoulis, C.: TEMORA-1:  
685 A new zircon standard for Phanerozoic U-Pb geochronology, *Chemical Geology*, 200, 155-170, 2003.
- 686
- 687 Black, L.P., Kamo, S.L., Allen, C.M., Davis, D.W., Aleinikoff, J.N., Valley, J.W., Mundil, R., Campbell, I.H.,  
688 Korsch, R.J., Williams, I.S., and Foudoulis, C.: Improved 206Pb/235U microprobe geochronology by the  
689 monitoring of a trace-element-related matrix effect; SHRIMP, ID-TIMS, ELA-ICP-MS and oxygen isotope  
690 documentation for a series of zircon standards, *Chemical Geology*, 205, 115-140, doi:  
691 <https://doi.org/10.1016/j.chemgeo.2004.01.003>, 2004
- 692
- 693 Bowring, J.F., McLean, N.M., and Bowring, S.A.: Engineering cyber infrastructure for U-Pb geochronology: Tripoli  
694 and U-Pb redux, *Geochemistry, Geophysics, and Geosystems*, 12, doi: <https://doi.org/10.1029/2010GC003479>, 2011
- 695
- 696 Carrapa, B., 2010: Resolving tectonic problems by dating detrital minerals, *Geology*, 38, 191–92, doi:  
697 <https://doi.org/10.1130/focus022010.1>, 2010
- 698
- 699 Chakoumakos, B.C., Murakami, T., Lumpkin, G.R., and Ewing, R.C.: Alpha-decay induced fracturing in zircon:  
700 The transition from the crystalline to metamict state, *Science*, 236, 1556-1559, 1987.
- 701
- 702 Condon, D.J., Schoene, B., McLean, N.M., Bowring, S.A., and Parrish, R.R.: Metrology and traceability of U-Pb  
703 isotopic dilution geochronology (EARTHTIME tracer calibration part 1), *Geochimica et Cosmochimica Acta*, 164,  
704 464-480, 2015
- 705
- 706 Coutts, D.S., Matthews, W.A., and Hubbard, S.M.: Assessment of widely used methods to derive depositional ages  
707 from detrital zircon populations, *Geoscience Frontiers*, 10, 1421-1435, 2019.
- 708
- 709 Crowley J.L., Schoene, B., and Bowring, S.A: U–Pb dating of zircon in the Bishop  
710 Tuff at the millennial scale, *Geology*, 35, 1123–1126, doi: <https://doi.org/10.1130/G24017A.1>, 2007
- 711
- 712 Crowley, Q.G., Heron, K., Riggs, N., Kamber, B., Chew, D., McConnell, B., and Benn, K.: Chemical Abrasion  
713 Applied to LA-ICP-MS U-Pb Zircon Geochronology, *Minerals*, 4, 503-518, doi:  
714 <https://doi.org/10.3390/min4020503>, 2014
- 715
- 716 Dickin, A.P.: Radiogenic Isotope Geology, 2<sup>nd</sup> Ed., Cambridge, UK: Cambridge University Press, 2005.
- 717
- 718 Dickinson, W.R., and Gehrels, G.E.: Use of U-Pb ages of detrital zircons to infer maximum depositional ages of  
719 strata: a test against a Colorado Plateau Mesozoic database, *Earth and Planetary Science Letters*, 288, 115-125,  
720 2009.
- 721
- 722 Eddy, M.P., Ibañez-Mejia, M., Burgess, S.D., Coble, M.A., Cordani, U.G., DesOrmeau, J., Gehrels, G.E., Li, X.,  
723 MacLennan, S., Pecha, M., Sato, K., Schoene, B., Valencia, V.A., Vervoort, J.D., and Wang, T.: GHR1 Zircon – A

724 New Eocene Natural Reference Material for Microbeam U-Pb Geochronology and Hf Isotopic Analysis of Zircon,  
725 *Geostandards and Geoanalytical Research*, 43, 113-132, doi: <https://doi.org/10.1111/ggr.12246>, 2019.  
726

727 Ewing, R.C., Meldrum, A., Wang, L., Weber, W.J., Corrales, I.R.: Radiation effects in zircon *In* Hanchar, J.M.,  
728 Hoskin, P.W.O. (Eds.), *Zircon. Rev. Mineral. Geochem.*, 53, *Mineral Society of America*, 277-303, 2003.  
729

730 Fedo C.M., Sircombe, K., and Rainbird, R.: Detrital zircon analysis of the sedimentary record, *Reviews in*  
731 *Mineralogy and Geochemistry*, 53, 277-303, doi: <https://doi.org/10.2113/0530277>, 2003  
732

733 Garver, J.I., and Kamp, P.J.J.: Integration of zircon color and zircon fission track zonation patterns in orogenic belts:  
734 Application of Southern Alps, New Zealand, *Tectonophysics*, 349, 203-219, 2002.  
735

736 Gehrels, G.E.: Detrital zircon U-Pb geochronology: current methods and new opportunities, *In Tectonics of*  
737 *Sedimentary Basins: Recent Advances*, eds C., Busby, A., Azor, pp. 47–62, Chichester, UK: Wiley-Blackwell, 2012  
738

739 Gehrels, G.E., Valencia, V., Ruiz, J.: Enhanced precision, accuracy, efficiency, and spatial resolution of U-Pb ages  
740 by laser ablation–multicollector–inductively coupled plasma–mass spectrometry, *Geochemistry, Geophysics, and*  
741 *Geosystems*, 9, doi: <https://doi.org/10.1029/2007GC001805>, 2008  
742

743 Gehrels, G.E.: Detrital zircon U-Pb Geochronology Applied to Tectonics: *Annual Review of Earth and Planetary*  
744 *Sciences*, 42, 127-149, doi: <https://doi.org/10.1146/annurev-earth-050212-124012>, 2014  
745

746 Gehrels, G.E., and Pecha, M.: Detrital zircon U-Pb geochronology and Hf isotope geochemistry of Paleozoic and  
747 Triassic passive margin strata of western North America, *Geosphere*, 10, 49–65, doi:  
748 <https://doi.org/10.1130/GES00889.1>, 2014  
749

750 Gehrels, G.E., Valencia, V., Pullen, A.: Detrital zircon U-Pb geochronology by Laser-Ablation Multicollector  
751 ICPMS at the Arizona LaserChron Center, in Loszewski, T., and Huff., W., eds., *Geochronology: Emerging*  
752 *Opportunities*, Paleontology Society Short Course: Paleontology Society Papers, 11, 2006.  
753

754 Ginster, U., Reiners, P.W., Nasdala, L., and Chanmuang C.N.: Annealing kinetics of radiation damage in zircon,  
755 *Geochimica et Cosmochimica Acta*, 15, 225-246, 2019.  
756

757 Goldich, S.S., and Mudrey, Jr., M.G.: Dilatancy model for discordant U-Pb zircon ages, In: A.I. Tugarinov (ed),  
758 *Contributions to Recent Geochemistry and Analytical Chemistry (Vinogradov Volume)*, 415-418, 1972.  
759

760 Herriot, T.M., Crowley, J.L., Schmitz, M.D., Marwan, W.A., and Gillis, R.J.: Exploring the law of detrital zircon:  
761 LA-ICP-MS and CA-TIMS geochronology of Jurassic forearc strata, Cook Inlet, Alaska, USA, *Geology*, 47, 1044-  
762 1048: <https://doi.org/10.1130/G46312.1>, 2019  
763

764 Hay, D.C., and Dempster, T.J.: Zircon alteration, formation, and preservation in sandstones, *Sedimentology*, 56,  
765 2175-2191, doi: 10.1111/j.1365-3091.2009.01075.x, 2009.  
766

767 Hay, D.C., and Dempster, T.J.: Zircon behaviour during low temperature metamorphism, *Journal of Petrology*, 50,  
768 571-598, 2009.  
769

770 Hiess, J., Condon, D. J., McLean, N. and Noble, S. R.:  $^{238}\text{U}/^{235}\text{U}$  Systematics in Terrestrial Uranium-Bearing  
771 Minerals, *Science*, 335, 1610–1614, 2012  
772

773 Hietpas, J., Samson, S., Moecher, D., Chakraborty, S.: Enhancing tectonic and provenance information from detrital  
774 zircon studies: assessing terrane-scale sampling and grain-scale characterization, *J. Geol. Soc. Lond.*, 168, 309-318,  
775 2011.  
776

777 Ibañez-Mejía, M., Pullen, A., Pepper, M., Urbani, F., Ghoshal, G., and Ibañez-Mejía, J.C.: Use and abuse of detrital  
778 zircon U-Pb geochronology – A case from the Rio Orinoco delta, eastern Venezuela, *Geology*, 46, 1019-1022, 2018.  
779

780 Jaffey, A.H., Flynn, K.F., Glendenin, L.E., Bentley, W.C., and Essling, A.M.: Precision Measurement of Half-Life  
781 and Specific Activities of  $^{235}\text{U}$  and  $^{238}\text{U}$ , *Physical Review C*, 4, 1971.  
782

783 Keller, C.B., Boehnke, P., Schoene, B., and Harrison, M.: Stepwise chemical abrasion-isotope dilution-thermal  
784 ionization mass spectrometry with trace element analysis of microfractured Hadean zircon, *Geochronology*, 1, 85-  
785 97, 2019.  
786

787 Kramers, J., Frei, R., Newville, M., Kober, B., Villa, I.: On the valency state of radiogenic lead in zircon and its  
788 consequences, 261, 4-11, 2009.  
789

790 Malusa, M.G., Carter, A., Limoncelli, M., Villa, I. M., and Garzanti, E.: Bias in detrital zircon geochronology and  
791 thermochronometry, *Chemical Geology*, 359, 90-107, 2013.  
792

793 Marsellos, A.E., and Garver, J.J.: Radiation damage and uranium concentration in zircon as assessed by Raman  
794 spectroscopy and neutron irradiation, *American Mineralogist*, 95, p. 1192-1201, 2010.  
795

796 Mattinson, J.M., A study of complex discordance in zircons using step-wise dissolution techniques, *Contributions to*  
797 *Mineralogy and Petrology*, 116, 117-129, 1994.  
798

799 Mattinson J.M.: Zircon U–Pb chemical-abrasion ("CA-TIMS") method: Combined annealing and multi-step  
800 dissolution analysis for improved precision and accuracy of zircon ages, *Chemical Geology*, 220, 47–56, doi:  
801 <https://doi.org/10.1016/j.chemgeo.2005.03.011>, 2005  
802

803 Mattinson, J.M.: Analysis of the relative decay constants of  $^{235}\text{U}$  and  $^{238}\text{U}$  by multi-step CA-TIMS measurements  
804 of closed system natural zircon samples, *Chemical Geology*, 275, 186-198, doi:  
805 <https://doi.org/10.1016/j.chemgeo.2010.05.007>, 2010  
806

807 McConnell, B., Riggs, N., and Crowley, Q.G.: Detrital zircon provenance and Ordovician terrane amalgamation,  
808 western Ireland, *Journal of the Geological Society*, 166, 473–484, doi: <https://doi.org/10.1144/0016-76492008-081>,  
809 2009  
810

811 McKanna, A.J., Koran, I., Schoene, B., and Ketcham, R.A.: Chemical abrasion: the mechanics of zircon dissolution,  
812 *Geochronology*, 5, 127-151, <https://doi.org/10.5194/gchron-5-127-2023>, 2023  
813

814 McLean, N.M., Condon, D.J., Schoene, B., and Bowring, S.A.: Evaluating uncertainties in the calibration of isotopic  
815 reference materials and multi-element isotopic tracers (EARTHTIME tracer calibration II), *Geochimica et*  
816 *Cosmochimica Acta*, 164, 481-501., 2015  
817

818 Mundil, R., Ludwig, K.R., Metcalfe, I., and Renne, P.R.: Age and timing of the Permian mass extinctions: U/Pb  
819 dating of closed-system zircons, *Science*, doi: 10.1126/science.1101012., 2004  
820

821 Nasdala, L., Hanchar, J.M., Kronz, A., Whitehouse, M.J.: Long-term stability of alpha particle damage in natural  
822 zircon, *Chemical Geology*, 220, 83-103, doi: <https://doi.org/10.1016/j.chemgeo.2005.03.012>, 2005  
823

824 Nemchin, A., and Cawood, P.: Discordance of the U-Pb system in detrital zircons: Implication for provenance  
825 studies of sedimentary rocks, *Sediment Geol.*, **182**, 143–162, 2005  
826

827 Parrish, R.R., and Noble, S.R.: Zircon U–Th–Pb geochronology by isotope dilution –Thermal ionization mass  
828 spectrometry (ID-TIMS): In Hanchar JM and Hoskin PWO (eds.) Zircon, *Reviews in Mineralogy and Geochemistry*,  
829 53, 183–213, Washington, DC: Mineralogical Society of America, 2003  
830

831 Pullen., A., Ibañez-Mejia, M., Gehrels, G.E., Ibanez-Mejia, J.C., and Pecha, M.: What happens when n=1000?  
832 Creating large-n geochronological datasets with LA-ICP-MS for geologic investigations, *Journal of Analytical*  
833 *Spectrometry*, 6, doi: <https://doi.org/10.1039/C4JA00024B>, 2014  
834



835 Pullen, A., Ibañez-Mejia, M., Gehrels, G.E., Giesler, D., and Pecha, M.: Optimization of a Laser Ablation-Single  
836 Collector-Inductively Coupled Plasma-Mass Spectrometer (Thermo Element 2) for Accurate, Precise, and Efficient  
837 Zircon U-Th-Pb Geochronology, *Geochemistry, Geophysics, and Geosystems*, 19, 3689-3705, 2018.  
838

839 Rahn, M.K., Brandon, M.T., Batt, G.E., Garver, J.I.: A zero damage model for fission-track annealing in zircon, *Am.*  
840 *Mineral*, 89, 473-484, 2004.  
841

842 Reiners, P.W.: Zircon (U-Th)/He Thermochronometry, *Reviews in Mineralogy & Geochemistry*, 58, 151-179, 2005.  
843

844 Satkoski, A.M., Wilkinson, B.H., Hietpas, J., and Samson, S.D.: Likeness among detrital zircon populations – An  
845 approach to the comparison of age frequency data in time and space, *Geological Society of America Bulletin*, 125,  
846 1783-1799, 2013.  
847

848 Saylor, J.E., and Sundell, K.E.: Quantifying comparison of large detrital geochronology data sets, *Geosphere*, 12, 1-  
849 18, 2016.  
850

851 Schaltegger, U., Schmitt, A.K., and Horstwood, M.S.A.: U-Th-Pb zircon geochronology by ID-TIMS, SIMS, and  
852 laser ablation ICP-MS: recipes, interpretations, and opportunities, *Chem. Geol.*, 402, 89-110,  
853 <https://doi.org/10.1016/j.chemgeo.2015.02.028>, 2015  
854

855 Schmitz, M.D., and Bowring, S.A.: U-Pb zircon and titanite systematics of the Fish Canyon Tuff: an assessment of  
856 high-precision U-Pb geochronology and its application to young volcanic rocks, *Geochimica et Cosmochimica Acta*,  
857 65, 2571-2587, 2001  
858

859 Schoene, B.: U-Th-Pb Geochronology, Treatise on geochemistry 2<sup>nd</sup> edition, doi: [http://dx.doi.org/10.1016/B978-0-  
860 08-095975-7.00310-7](http://dx.doi.org/10.1016/B978-0-08-095975-7.00310-7), 2014  
861

862 Sharman, G.R., and Malkowski, M.A.: Needles in a haystack: Detrital zircon U-Pb ages and the maximum  
863 depositional age of modern global sediment, *Earth Science Reviews*, 203, 2020  
864

865 Smith, T.M., Saylor, J.E., Lapen, T.J., Leary, R.J., and Sundell, K.E.: Large detrital zircon data set investigation and  
866 provenance mapping: Local versus regional and continental sediment sources before, during, and after Ancestral  
867 Rocky Mountain deformation, *GSA Bulletin*, doi: <https://doi.org/10.1130/B36285.1>, 2023  
868

869 Sláma, J., Kosler, J., Condon, D.J., Crowley, J.L., Gerdes, A., Hanchar, J.M., Horstwood, M.S.A., Morris, G.A.,  
870 Nasdala, L., Norberg, N., Schaltegger, U., Schoene, B., Tubrett, M.N., and Whitehouse, M.J.: Plesovice zircon – A  
871 new natural reference material for U-Pb and Hf isotopic microanalysis, *Chemical Geology*, 249, 1-35, doi:  
872 <https://doi.org/10.1016/j.chemgeo.2007.11.005>, 2008  
873

874 Slama, J., and Kosler, J.: Effects of sampling and mineral separation on accuracy of detrital zircon studies,  
875 *Geochemistry, Geophysics, Geosystems*, 13, 2012.  
876

877 Stern, R.A., Bodorkos, S., Kama, S.L., Hickman, A.H., and Corfu, F.: Measurement of SIMS instrumental mass  
878 fractionation of Pb isotopes during zircon dating, *Geostandards and Geoanalytical Research*, 33, 145-168, doi:  
879 <https://doi.org/10.1111/j.1751-908X.2009.00023.x>, 2009  
880

881 Sundell, K. E., Gehrels, G. E., and Pecha, M. E.: Rapid U-Pb Geochronology by Laser Ablation Multi-Collector  
882 ICP-MS, *Geostand Geoanal Res.*, 45, 37–57, 2021  
883

884 Vermeesch, P.: Maximum depositional age estimation revisited, *Geoscience Frontiers*, 12, 843-850, 2021.  
885

886 Von Quadt, A., Dallhofer, D., Guilong, M., Peytcheva, I., Waelle, M., and Sakata, S.: U-Pb dating of CA/non-CA  
887 treated zircons obtained by LA-ICP-MS and CA-TIMS techniques: impact for their geological interpretation,  
888 *Journal of Analytical Atomic Spectrometry*, 29, 1618-1629, doi: <https://doi.org/10.1039/C4JA00102H>, 2014  
889

890 Wang, J. W., Gehrels, G., Kapp, P. & Sundell, K.: Evidence for regionally continuous Early Cretaceous sinistral  
891 shear zones along the western flank of the Coast Mountains, coastal British Columbia, Canada, *Geosphere*, 19, 139–  
892 162, 2022.

893

894 Widmann, P., Davies, J.H.F.L., and Schaltegger, U.: Calibrating chemical abrasion: Its effects on zircon crystal  
895 structure, chemical composition and U-Pb age, *Chemical Geology*, 511, 1-10,  
896 <https://doi.org/10.1016/j.chemgeo.2019.02.026>, 2019

897

898 Wiedenbeck, M., Alle, P., Corfu, F., Griffin, W.L., Meier, M., Oberli, F., von Quadt, A., Roddick, J.C., and Spiegel,  
899 W.: Three natural zircon standards for U-Th-Pb, Lu-Hf, trace element and REE analyses, *Geostandards Newsletter*,  
900 v. 19, p. 1-23, 1995

901

902 Wiedenbeck, M., Hanchar, J.M., Peck, W.H., Sylvester, P., Valley, J., Whitehouse, M., Kronz, A., Morishita, Y.,  
903 Nasdala, L., Fiebig, J., Franchi, I., Girard, J.P., Greenwood, R.C., Hinton, R., Kita, N., Mason, P.R.D., Norman, M.,  
904 Ogasawara, M., Piccoli, P.M., Rhede, D., Satoh, H., Schultz-Dobrick, B., Skar, O., Spicuzza, M.J., Terada, K.,  
905 Tindle, A., Togashi, S., Vennemann, T., Xie, Q., and Zheng, Y.F.: Further characterization of the 91500 zircon  
906 crystal, *Geostandards and Geoanalytical Research*, v. 28, p. 9-39, doi: [https://doi.org/10.1111/j.1751-](https://doi.org/10.1111/j.1751-908X.2004.tb01041.x)  
907 [908X.2004.tb01041.x](https://doi.org/10.1111/j.1751-908X.2004.tb01041.x), 2004

908

909 Wotzlaw, J.F., Schaltegger, U., Frick, D.A., Dungan, M.A., Gerdes, A., and Gunther, D.: Tracking the evolution of  
910 large-volume silicic magma reservoirs from assembly to supereruption, *Geology*, 41, 867-870, 2013

911